Quaternary Science Reviews 136 (2016) 209–228

Contents lists available at ScienceDirect

Quaternary Science Reviews

journal homepage: www.elsevier.com/locate/quascirev

Climate variability and socio-environmental changes in the northern Aegean (NE Mediterranean) during the last 1500 years

Alexandra Gogou [a, *], Maria Triantaphyllou [b], Elena Xoplaki [c], Adam Izdebski [d], Constantine Parinos [a], Margarita Dimiza [b], Ioanna Bouloubassi [e], Juerg Luterbacher [c], Katerina Kouli [b], Belen Martrat [f], Andrea Toreti [g], Dominik Fleitmann [h], Gregory Rousakis [a], Helen Kaberi [a], Maria Athanasiou [b], Vasilios Lykousis [a]

[a] Hellenic Centre for Marine Research, Institute of Oceanography, 190 13 Anavyssos, Attiki, Greece
[b] Faculty of Geology and Geoenvironment, University of Athens, Panepistimioupolis, 157 84 Athens, Greece
[c] Justus-Liebig-University Giessen, Department of Geography, Climatology, Climate Dynamics and Climate Change, Senckenbergstr. 1, 35390 Giessen, Germany
[d] Jagiellonian University in Krakow, Institute of History, Gołębia 13, 31-007 Kraków, Poland
[e] Laboratoire d'Océanographie et du Climat, Expérimentation et Approche Numérique, Université Pierre et Marie Curie, Paris Cedex 05, France
[f] Department of Environmental Chemistry, Spanish Council for Scientific Research (IDÆA-CSIC), 08034 Barcelona, Spain
[g] European Commission, Joint Research Centre, Ispra, Italy
[h] Department for Archaeology and Centre for Past Climate Change, School of Archaeology, Geography and Environmental Science, Whiteknights, University of Reading, RG6 6AB Reading, United Kingdom

ARTICLE INFO

Article history:
Received 6 April 2015
Received in revised form
10 January 2016
Accepted 13 January 2016
Available online 5 February 2016

Keywords:
Alkenone-SST
Mediterranean sea
Aegean sea
Proxy-reconstructions
MCA
LIA
Tambora eruption
Societal impacts of climate change

ABSTRACT

We provide new evidence on sea surface temperature (SST) variations and paleoceanographic/paleo-environmental changes over the past 1500 years for the north Aegean Sea (NE Mediterranean). The reconstructions are based on multiproxy analyses, obtained from the high resolution (decadal to multi-decadal) marine record M2 retrieved from the Athos basin. Reconstructed SSTs show an increase from ca. 850 to 950 AD and from ca. 1100 to 1300 AD. A cooling phase of almost 1.5 °C is observed from ca. 1600 AD to 1700 AD. This seems to have been the starting point of a continuous SST warming trend until the end of the reconstructed period, interrupted by two prominent cooling events at 1832 ± 15 AD and 1995 ± 1 AD. Application of an adaptive Kernel smoothing suggests that the current warming in the reconstructed SSTs of the north Aegean might be unprecedented in the context of the past 1500 years. Internal variability in atmospheric/oceanic circulations systems as well as external forcing as solar radiation and volcanic activity could have affected temperature variations in the north Aegean Sea over the past 1500 years. The marked temperature drop of approximately ~2 °C at 1832 ± 15 yr AD could be related to the 1809 AD 'unknown' and the 1815 AD Tambora volcanic eruptions. Paleoenvironmental proxy-indices of the M2 record show enhanced riverine/continental inputs in the northern Aegean after ca. 1450 AD.

The paleoclimatic evidence derived from the M2 record is combined with a socio-environmental study of the history of the north Aegean region. We show that the cultivation of temperature-sensitive crops, i.e. walnut, vine and olive, co-occurred with stable and warmer temperatures, while its end coincided with a significant episode of cooler temperatures. Periods of agricultural growth in Macedonia coincide with periods of warmer and more stable SSTs, but further exploration is required in order to identify the causal links behind the observed phenomena. The Black Death likely caused major changes in agricultural activity in the north Aegean region, as reflected in the pollen data from land sites of Macedonia and

* Corresponding author. Hellenic Centre for Marine Research, Institute of Oceanography, 190 13 Anavyssos, Attiki, Greece.
E-mail addresses: agogou@hcmr.gr (A. Gogou), mtriant@geol.uoa.gr (M. Triantaphyllou), Elena.Xoplaki@geogr.uni-giessen.de (E. Xoplaki), adam.izdebski@fundusz.org (A. Izdebski), mdimiza@geol.uoa.gr (M. Dimiza), ioanna.bouloubassi@locean-ipsl.upmc.fr (I. Bouloubassi), Juerg.Luterbacher@geogr.uni-giessen.de (J. Luterbacher), akouli@geol.uoa.gr (K. Kouli), belen.martrat@idaea.csic.es (B. Martrat), andrea.toreti@jrc.ec.europa.eu (A. Toreti), d.fleitmann@reading.ac.uk (D. Fleitmann).

http://dx.doi.org/10.1016/j.quascirev.2016.01.009
0277-3791/

the M2 proxy-reconstructions. Finally, we conclude that the early modern peaks in mountain vegetation in the Rhodope and Macedonia highlands, visible also in the M2 record, were very likely climate-driven.

1. Introduction

The Mediterranean Sea is a semi-enclosed basin situated in a climatic transition zone between tropical and mid-latitude climates, making it highly sensitive to the global climate change (e.g., Corte-Real et al., 1995; Ribera et al., 2000; Xoplaki et al., 2003a; b; Lionello et al., 2006). This sensitivity is largely attributed to its small size, the limited connection to the Atlantic Ocean and its nearly independent thermohaline circulation, that causes a more immediate and amplified response to climatic variability (Lionello et al., 2006 and references therein).

The climate of the Mediterranean Basin is influenced by large-scale atmospheric circulation patterns and complex land–sea and basin-orography interactions (e.g., Corte-Real et al., 1995). Atmospheric modes of variability, such as the Arctic Oscillation/North Atlantic Oscillation (AO/NAO), the East Atlantic (EA), the East Atlantic/Western Russian (EA/WR) patterns and the El Nino Southern Oscillation (ENSO) play an important role on seasonal temperature and precipitation variability, as well as on surface water heat fluxes that in turn have influence on the Mediterranean thermohaline circulation (Xoplaki et al., 2003a,b, 2004; Brönnimann et al., 2007; Josey et al., 2011; López-Parages and Rodríguez-Fonseca, 2012; Malanotte-Rizzoli et al., 2014 and references therein). Recent studies (Josey et al., 2011; Skliris et al., 2012; Kontoyiannis et al., 2012; Papadopoulos et al., 2012) have discussed the role of the North Atlantic/European atmospheric variability modes on heat fluxes and deep-water convection in the Mediterranean basin, in particular during winter when cold winds cause important heat losses and stratification breakdown. Following this mechanism, strong interactions with the atmosphere induce winter mixing in the Gulf of Lions and/or in the Adriatic Sea (Malanotte-Rizzoli et al., 2014; Pinardi et al., 2015; and references therein). Temporarily deep-water formation has also been reported in the Aegean Sea during the late 1980s to early-mid 1990s, under the influence of anomalously cold winters, known as the Eastern Mediterranean transient (EMT) (Roether et al., 1996; Theocharis et al., 1999, 2014).

The Mediterranean experienced marked climatic, environmental and oceanographic changes in the past, often closely related to the northern hemisphere and the global scale variability (Luterbacher et al., 2012; Rohling et al., 2015). Marked changes in Mediterranean climate during the last two millennia have been described in the literature (Luterbacher et al., 2012; and references therein) and can be summarized as follow: a cold interval (Dark Ages Cold Period; DA) from 300 to 600 AD with a marked drop in temperatures at 450 AD, a period from 600 to 1200 AD (Medieval Climate Anomaly; MCA) characterized by warmer conditions, but interrupted by two cooler events at 700 and 1100 AD. Finally, the period from 1200 to 1850 AD, known as 'Little Ice Age' (LIA), with cooling extremes occurring at around 1400 AD and 1625 AD.

Based on current knowledge on the Mediterranean region, the first six centuries AD included some of the most intense and long-lasting droughts of the late Holocene in the Middle Eastern region (Roberts et al., 2012). High-resolution paleolimnological data from the Iberian peninsula show good inter-site coherence and indicate lower water levels and higher salinities synchronous with the MCA and generally more humid conditions during the LIA (Roberts et al., 2012). This pattern is in agreement with other lake, marine and tree ring records from Iberia and Morocco (Esper et al., 2007). In contrast, lake and partly speleothem evidence from Turkey shows an opposite pattern of a wet MCA and a dry LIA (Roberts et al., 2012 and references therein). According to the latter study, an east-west climate seesaw seems to have operated between the two Mediterranean sub-basins for the last 1.1 kyrs, showing that the eastern Mediterranean experienced generally drier hydro-climatic conditions during the LIA and a wetter phase during the MCA. However, while western Mediterranean aridity/humidity patterns appear consistent during the two periods, the pattern is less clear in the eastern Mediterranean region (Roberts et al., 2012). This is in agreement with recent tree ring based drought/wetness reconstructions for the Mediterranean (Cook et al., 2015; 2016).

Luterbacher et al. (2004); Xoplaki et al. (2005); Pauling et al. (2006), Lelieveld et al. (2012); Cook et al. (2015; 2016) and Luterbacher et al. (2016) present seasonal climate reconstructions for the last centuries covering the eastern Mediterranean. Seasonal information for the area is scattered and information about variability, trends and extremes at intraseasonal and interannual scale have therefore large uncertainties (Luterbacher et al., 2012). Marked fluctuations in seasonal temperatures are also related to large tropical volcanic eruptions. Wagner and Zorita (2005) indicated that on global and hemispheric scales, the volcanic forcing was largely responsible for the temperature drop during the Dalton solar minimum (period of reduced sunspot activity that occurred between ca. 1790 and 1830 AD), whereas changes in solar forcing and the increasing atmospheric CO_2 concentrations were of minor importance. The net effect of explosive volcanism is thought to be a cooling of global near-surface temperatures (Robock and Jianping, 1995), but regional deviations might occur, particularly during winter and summer (e.g., Fischer et al., 2007; Esper et al., 2013; Wegmann et al., 2014; Büntgen et al., 2015).

A recent review of the Mediterranean climate variability for the last two millennia (2K), stressed the lack of high temporal resolution/continuous SST records, especially from the eastern Mediterranean sub-basin (Luterbacher et al., 2012). Marine records combining marine and terrestrial proxies can provide valuable information by testing the synchronicity of proxy-events in land and ocean. Moreover, this approach can help to overcome dating issues of using different archives, and unambiguously resolve the land-sea interactions during the study interval.

Here we present a decadal to multi-decadal SST reconstruction over the past 1500 years in the north Aegean (northeastern Mediterranean), based on the study of alkenone paleothermometry and a plethora of organic geochemical, micropaleontological and pollen proxy-indices obtained from the marine multi-core M2 (Fig. 1). We compare fluctuations in the M2 mean SST reconstruction with independent paleoclimatic evidence from other reconstructions of marine and continental records from the Mediterranean and the Anatolian regions. During most of the last two millennia, the north Aegean region remained densely populated and it was one of the core areas of the Byzantine (4th–15th c.) and Ottoman (15th–19th c.) empires, from which there is a substantial amount of historical and archaeological data. That enables us to put societal developments that took place around the north Aegean Sea during the time frame of the M2 record into a climate context. The eastern Mediterranean region bears a long history of human development making it a focal point for exploring the complex interactions

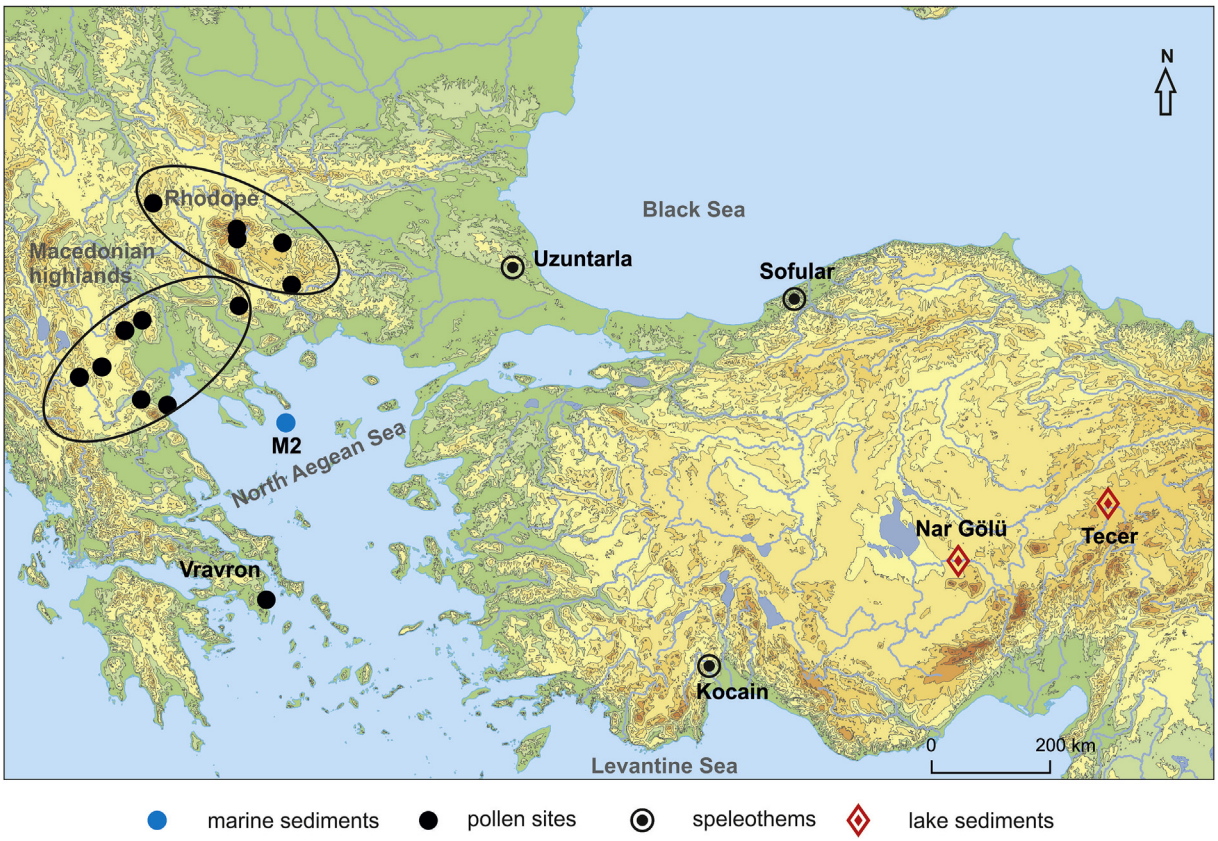

Fig. 1. Study area map of the north Aegean Sea (northeastern Mediterranean, Greece). The M2 sampling site location, pollen sites from Macedonia and the adjoining Rhodope mountains (for details on terrestrial pollen sites see Table 1) and continental sites (lakes, speleothems) from the Anatolia region.

between climate (including atmospheric and oceanic forcings), environment and human activity on time scales ranging from decadal to multi-centennial (e.g., deMenocal, 2001; Robinson et al., 2006; Roberts et al., 2011; Luterbacher et al., 2012; Medina-Elizalde and Rohling, 2012; Borrell et al., 2015; Berger et al., 2016; Weiberg et al., 2016; Xoplaki et al., 2016).

2. Regional setting

2.1. Oceanographic setting

The Aegean Sea is connected with the Black and Marmara Seas through the Dardanelles Straits, and with the open eastern Mediterranean (Levantine Sea) through the Cretan Straits (Fig. 1). The basin exhibits a complicated physical and geographic configuration, displaying complicated seabed morphology and numerous island complexes (Lykousis et al., 2002). Numerous major rivers (catchments > 1000 km^2) from the surrounding areas of the Balkans and Turkey flow into the Aegean Sea. Evros, Nestos and Strymon rivers discharge into the Aegean Sea, collectively constituting an important source of land-derived organic matter (Fig. 1). Black Sea waters (BSW) and riverine inputs both supply the northern Aegean with freshwater inputs (Poulos et al., 1997; Roussakis et al., 2004; Triantaphyllou et al., 2016), with the BSW inflow rate showing strong seasonal and interannual variability, reaching its maximum during mid to late summer and its minimum during winter (Zervakis et al., 2000).

The north Aegean Sea is one of the dense water formation areas in the Mediterranean (e.g., Theocharis and Georgopoulos, 1993; Lascaratos et al., 1999; Zervakis et al., 2000; 2003; Velaoras and Lascaratos, 2005; Gertman et al., 2006; Androulidakis et al., 2012). BSW spreading during winter may result in the stratification of the water column, thus influencing dense water formation activity (Zervakis et al., 2000; Zervakis et al., 2004; Velaoras and Lascaratos, 2010; Velaoras et al., 2013).

The spatial distribution of the Mediterranean annual SSTs is presented in Fig. 2. The average annual value of the Aegean basin SSTs where core M2 was retrieved is 18.2 °C (Kaplan SST V2, Kaplan et al., 1998; Bottomley et al., 1990; Reynolds and Smith, 1994; Parker et al., 1995).

2.2. Historical setting and potential for the socio-environmental study

The regions considered herein are Macedonia and the adjoining Rhodope mountains, in particular the Pirin mountain range which is located close to both the Macedonian lowlands and the North Aegean (Fig. 1). During the last two thousand years, these two regions developed along parallel trajectories. The Macedonian plain and its surrounding areas (hills to the north-west, the Chalkidike peninsula to the south, and the Strymon valley to the east; Fig. 1) were the primary focus for plant cultivation, manufacturing activities and commerce. The highlands and mountains of Rhodope were primarily engaged in pastoral economies, and depended for both supply and trade of its products on the core area of Macedonia (Izdebski et al., 2015). Archaeological data for Macedonia is available in greater quantity for most of Antiquity (especially for its later part, until ca. 600 AD), allowing to analyse the long-term settlement patterns in close detail (Dunn, 1994; 2005; Curta, 2012). Moreover, due to the economic and military importance of the city of Thessaloniki, Macedonia features in numerous medieval Byzantine texts (from at least the 5th c. until as late as the 15th c.-

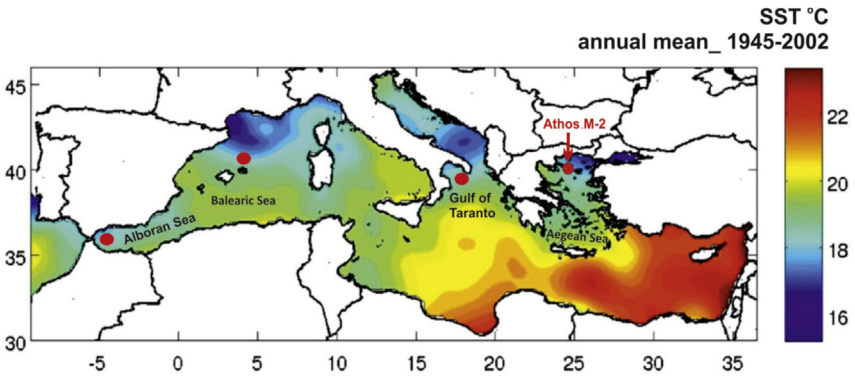

Fig. 2. Map showing the locations of the study core M2 retrieved from the Athos basin of the North Aegean (NE Mediterranean, this study) and of cores retrieved from the Central (Gulf of Taranto, Grauel et al., 2013) and Western Mediterranean Seas (Alboran Sea, Nieto-Moreno et al., 2013; Balearic Sea, Moreno et al., 2012). Mean SSTs calculated from 1945 to 2002 period using the MEDAR/MEDATLAS 2002 database (Fichaut et al., 2003).

e.g., Lemerle, 1979; Odorico, 2005). Most importantly, from the 10th c. onwards there exists a growing amount of archival evidence, coming first from the Athos monastic archives (covering primarily the Chalkidike and the Strymon valley, as well as the islands of Lemnos and Thasos; other archives include those of the Patmos monastery) and since the late 15th c. from the Ottoman registers (Lefort, 1986). This continuous availability of relatively detailed historical evidence makes Macedonia unique among all the other regions of the Balkans and Anatolia, where very little or simply nothing had been preserved from the medieval archival material. Last but not least, when we consider the high concentration of relatively well-dated pollen sites in both the hills surrounding the Macedonian plain, and in the Rhodope, in particular in the Pirin Mountains (Izdebski, in press; Marinova et al., 2012), it becomes clear that this part of the Byzantine and later Ottoman empires is very well suited for a detailed study of the socio-environmental history.

Pollen data from the Macedonian highlands and Rhodope have been analyzed for regional patterns of vegetation change during the last two thousand years (Izdebski et al., 2015; for site locations and data see Fig. 1 and Table 1). The regional pollen curves represent average proportionate values for specific pollen taxa (expressed in percentage values); averages have been weighted both for the reliability of a site age-depth model (arbitrary weights) and for the spatial and temporal structure of the site data that form each of the region (endogenous weights). The method of quantitative analysis is described in detail in a separate methodological paper (Izdebski et al., 2016). It should be noted, however, that only the Rhodope can be considered as a source area for the delivery of pollen and other terrestrial contents to the Athos basin (site of the M2 marine record), while the Macedonian highlands region is not considered as M2 site's primary source area. Nevertheless, the climatic and anthropogenic influence on the vegetation history recorded in the regional pollen data for the Macedonian highlands can be compared with the M2 climatic reconstructions, which provide information about the changing climatic conditions (e.g. temperature and humidity) in the entire north Aegean region.

Table 1
Pollen sites from Macedonia and Rhodope included in the quantitative analyses of the regional vegetation histories discussed in section 5.4 of this paper. Data source: EPD. Information regarding the original site publications, the data processing and the adopted age-depth models: Izdebski et al., 2015.

Site name	Elevation	Latitude	Longitude
Macedonian highlands			
Litochoro	25 m	40.138	22.546
Flambouro	1645 m	40.259	22.171
Orestias	630 m	40.500	21.250
Khimaditis Ib	560 m	40.616	21.583
Mount Voras	1640 m	41.020	21.910
Mount Paiko	1080 m	41.052	22.275
Lailias	1420 m	41.266	23.600
Rhodope (Western Bulgaria)			
Popovo Ezero	2185 m	41.716	23.666
Elatia-Rhodopes	1520 m	41.479	24.326
Besbog	2240 m	41.750	23.666
Beliya Kanton	1547 m	41.733	24.133
Begbunar	1750 m	42.150	22.550
Sredna Gora Mountains Peat Bog	1300 m	42.833	24.833

3. Methodology

3.1. Core location and description

The multicore M2 was retrieved in 2010 from the north Aegean Sea, Greece (Athos basin, 40° 05.15′N, 24° 32.68′E) onboard the R/V 'Aegaeo' during the 'MEDECOS II' cruise at a water depth of 1018 m (Fig. 1A). The 48-cm long core was sampled continuously at a sampling step of 0.5 cm. Sediments consist largely of olive grey (2.5GY 5/1) to greyish olive (5Y 5/2) homogeneous mud, with high silt contents (25–45%); the clay mineral assemblage comprises mainly of illite ranging between 40 and 60% of the total material (lithologic unit A; Roussakis et al., 2004).

3.2. Chronology

An age-depth model has been constructed by combining ^{210}Pb dates and accelerator mass spectrometry (AMS) ^{14}C dates (Table 2). ^{210}Pb measurements were performed on the upper 10 cm at a step of 0.5 cm; the resolution became 1 cm until 20 cm depth, and increased up to 5–10 cm until 40 cm depth. ^{210}Pb activities were determined through the measurement of its a-emitting granddaughter ^{210}Po (Sanchez-Cabeza et al., 1998). The dried sediments were leached successively with HNO_3, HNO_3–$HClO_4$, HF and HCl and ^{210}Po isotopes were deposited on silver discs and counted on a total a-counter (Ortec EG&G) (Radakovitch, 1995). Repeated measurements on a number of sediment samples showed an analytical precision better than 5%. The ^{226}Ra-supported ^{210}Pb (background) was assumed to be 36 Bq/kg, a value measured in the deeper part of the core (36 cm). The down-core total ^{210}Pb activity profile is presented in Fig. 3A. The activity profile shows an upper interval (~10–11 cm) of rapid exponential-downward decline in ^{210}Pb activity, followed by a lower interval with constant activity. For the calculation of the sedimentation rates, the constant rate of supply (CRS; Appleby and Oldfield, 1978) sedimentation model has been used, as the Athos basin receives terrigenous supply from the north

Table 2
Age model pointers for the investigated core M2.

Depth (cm)	Material	^{14}C ages	cal year BP	cal year AD	Mean age	Error ±1σ
16.5–18.5 cm	planktonic forams	200±30[a]		1750	1750	21
23.5–25.5 cm	planktonic forams	760 ± 30	271–440	1510–1679	1594,5	60
30.5–32.5 cm	planktonic forams	950 ± 30	440–570	1380–1510	1445	46
41.5–43.4 cm	planktonic forams	1520 ± 30	919–1116	834–1031	932,5	70
46.5–48.5 cm	planktonic forams	1910 ± 30	1309–1496	454–641	547,5	66

[a] Result out of calibration range.

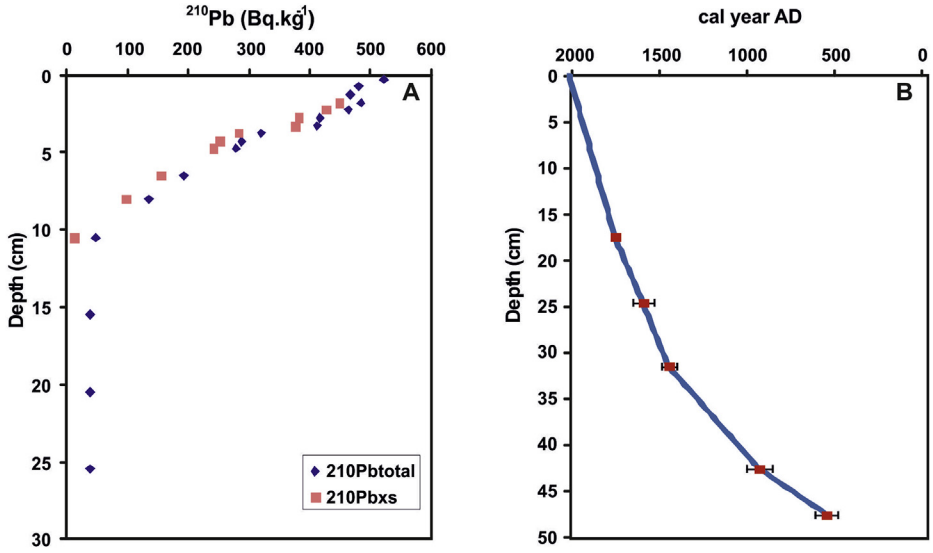

Fig. 3. Information used to construct age model. (A) ^{210}Pb activity downcore M2 core, and (B) depth vs. AD ages (with 1σ error) for M2 core.

Aegean borderland. Five accelerator mass spectrometry (AMS) ^{14}C dates were performed at the laboratories of Beta Analytic (USA) on cleaned hand-picked planktonic foraminifera (mostly *Globigerinoides ruber*). ^{14}C ages were converted into calibrated ages using the Calib v. 7.02 software (Reimer et al., 2013) and the MARINE13 calibration dataset, using the local marine reservoir age of 58 ± 85 years (Reimer and McCormac, 2002). The age model is based on linear interpolation between the ^{14}C dates and presented in Fig. 3B. A maximum sedimentation rate for the upper 10.5 cm of the sediment core was calculated using the CRS model at about 83 cm/kyr, thus close to the ~87 cm/kyr estimate derived from the ^{14}C dating for the 0–17 cm interval. Temporal resolution ranges from ~8 to 40 years, with higher temporal resolution during the LIA and last century than the MCA, as a result of lower sedimentation during the latter period. Thus, time resolution of the M2 record can be characterized as decadal to multi-decadal.

3.3. TOC and $\delta^{13}C_{org}$

Ninety six samples were collected at a resolution step of 0.5 cm for organic carbon (OC) content and $\delta^{13}C_{org}$ analysis, which were carried out at the University of California, Davis. Methods for OC content and $\delta^{13}C_{org}$ analysis have been previously reported in detail (Katsouras et al., 2010). Stable carbon isotope ratios were expressed in terms of $\delta^{13}C_{org}$ values against Vienna Pee Dee Belemnite (V-PDB), with an overall analytical error based on duplicate measurements estimated at ±0.2‰.

3.4. Organic geochemistry

The determination of lipid biomarkers was carried out on 96 samples. Lipids were extracted from freeze-dried sediments by sonication using a mixture of dichloromethane/methanol (4:1; v/v) and separated into different compound classes on silica gel column chromatography, using solvent mixtures of increasing polarity (modified after Gogou et al., 2007). Individual compounds were identified and quantified by GC–FID and GC–MS with a combination of comparison of GC retention times to authentic standards and comparison of their mass spectral data to those of the literature. Details regarding the analytical procedure are described in Gogou et al. (2007).

A range of selected lipid biomarkers were considered in this study, including certain long-chain *n*-alkanes and *n*-alkanols, long-chain alkenones with 37 and 38 carbon atoms, long-chain diols, the isoprenoid derivatives loliolide and isololiolide, and selected sterols. The detailed study of a variety of lipid biomarkers in paleoceanographic studies permits to both autochthonous and allochthonous sources contributing to the sedimentary organic matter, delivering information on marine and terrestrial ecosystem responses to climatic variability and land-ocean interactions (e.g. Hinrichs et al., 1999; Gogou et al., 2007; Strong et al., 2013; Ouyang et al., 2015 and references therein).

High molecular weight *n*-alkanes and *n*-alkanols are major components of epicuticular higher plant waxes (Eglinton and Hamilton, 1967; Eglinton and Eglinton, 2008) and have been often used as proxies of allochthonous natural (terrestrial) inputs from leaf waxes of higher plants (e.g., Ohkouchi et al., 1997; Gogou et al., 2007). The sum of the concentrations of the most abundant high molecular weight *n*-alkanes and *n*-alkanols of terrestrial origin are defined, respectively, as:

$$\mathrm{TerNA} = \sum n - C_{27,29,31}$$

and

$$\mathrm{TerNA-OH} = \sum n - C_{26,28,30}$$

The Carbon Preference Indices of long chain *n*-alkanes (CPI_{NA}) and *n*-alkanols (CPI_{N-OH}) have been used as indicators of terrestrial OM degradation with CPI values in fresh leaves being typically >4 (Ohkouchi et al., 1997), although the occurrence of petroleum hydrocarbons bias (lower) CPI_{NA} values with increasing petroleum contribution, since fossil fuel products present CPI_{NA} values ~1 (Wang et al., 1999). The indices were calculated, respectively, as:

$$\mathrm{CPI_{NA}} = \sum([n-C_{25}]-[n-C_{33}]) \Big/ \sum([n-C_{26}]-[n-C_{34}])$$

and

$$\mathrm{CPI_{N-OH}} = \sum([n-C_{24}]-[n-C_{30}]) \Big/ \sum([n-C_{23}]-[n-C_{29}])$$

Long-chain alkenones reflect the productivity from algal species of the *Prymnesiophyte* class, e.g., *Emiliania huxleyii* (Marlowe et al., 1984), while in general, the known biological precursors of long-chain diols are marine nannoplankton of the class *Eustigmatophyta* and C_{30} keto-ols might be deriving by oxidation of the corresponding C_{30} diols (Volkman, 1986 and references therein). However, long-chain diols have also been identified in *Proboscia* diatoms (Rampen et al., 2008; Rodrigo-Gamiz et al., 2014). Lolioliides (isololiolide and loliolide) share several structural features characteristic of carotenoids in marine algae, which were proposed to serve as their biogenic precursors (Repeta, 1989). Marine sterols are major constituents of several marine phytoplankton groups such as prymnesiophytes, diatoms and dinoflagellates (Volkman et al., 1999; Menzel et al., 2003). Sterols employed as marine biomarkers in this study consist of brassicasterol and dinosterol. Brassicasterol ($_{28}\Delta^{5,22E}$) is the major sterol in many diatoms but it also occurs in some prymnesiophytes, mainly *Emiliana huxleyi*, while dinosterol ($_{30}\Delta^{22E}$) is a major compound in dinoflagellates and is commonly used as source-specific biomarkers of this algal specie (Volkman, 1986; Volkman et al., 1999). The sum of the concentrations of the considered lipid biomarkers of algal origin was calculated as follows:

$$\sum \mathrm{Algal} = \sum \Big({}_{28}\Delta^{5,22E} + {}_{30}\Delta^{22E} + C_{30}\mathrm{diols\ \&\ keto-ols} + C_{37}\mathrm{alkenones} + \mathrm{loliolide} + \mathrm{iso-loliolide} \Big)$$

3.5. Coccolithophores

Preparation of samples, quantitative counting methods and taxonomy of coccolithophore analysis are described in detail elsewhere (Triantaphyllou et al., 2009a; b, 2014; Triantaphyllou, 2014). A total of 73 samples have been prepared for coccolithophore analyses. Sample preparation followed the standard smear slide techniques. Results are presented in relative abundances in order to avoid any dilution effects, e.g., terrigenous matter input (Flores et al., 1997). The lower photic zone species *Florisphaera profunda* has proven to be a reliable proxy of the nutricline–thermocline (Okada and Honjo, 1973; Molfino and McIntyre, 1990); thus, high relative abundances indicate stable stratification of the water column and low productivity in the surface layer (e.g., Castradori, 1993; Beaufort et al., 2001; Flores et al., 2000). *Emiliania huxleyi* is considered to be a proxy for high nutrient concentrations and increased productivity in surface waters (Young, 1994) and is a species that prevails during winter in the Aegean Sea (Dimiza et al., 2008; 2015). Relative maxima in the abundances of *Helicosphaera* spp. (mainly *Helicosphaera carteri*) together with *Braarudosphaera bigelowii* have been used as indicators of salinity decrease (e.g., Giunta and Negri, 2001; Colmenero-Hidalgo et al., 2004; Grelaud et al., 2012), whereas warm species % [*Rhabdosphaera* spp., *Syracosphaera* spp., *Umbellosphaera* spp. (mostly *U. tenuis*), *Umbilicosphaera sibogae, Calciosolenia* spp.] signal stratified and oligotrophic warm upper water column layers (e.g., Winter et al., 1994; Palumbo et al., 2013).

3.6. Pollen

Pollen sample preparation followed the protocol as used in marine cores from the Aegean Sea (Triantaphyllou et al., 2009a; Kouli et al., 2012). In total 37 samples were analyzed from the first 41 cm of the multicore. Samples below that level exhibited low pollen abundances and they were not used in this study. Pteridophyte spores and aquatic taxa were excluded from pollen sum.

Terrestrial palynomorphs of M2 sediment layers were mainly transported in the marine environment by fluvial transport and are expected to closely reflect the vegetation of eastern Macedonia, including Strymon valley, Rhodope and Athos Peninsula and to a lesser extend Thasos Island and Drama plain (Fig. 1B). Pollen data are summarized in the following groups: Altitudinal include *Abies, Picea* and *Fagus*. Other deciduous include *Alnus, Corylus, Acer, Fraxinus, Juglans, Ostrya, Platanus, Populus* and *Ulmus*. Mediterranean taxa include *Cistus, Quercus ilex, Phillyrea, Pistacia* and *Olea*. In the curve of Steppic taxa Artemisia, Chenopodiaceae and Asteraceae are included. A forestation index (F-Index), calculated as the ratio of the sum of broadleaved tree percentage versus pollen sum excluding bisaccates (Kotthoff et al., 2008; Kouli et al., 2012), has been used to evaluate the woodland cover. The OJC group (Olea, Juglans, Castanea: Mercuri et al., 2013a) and the anthropogenic pollen indicators sum (API; Mercuri et al., 2013b) are used in order to quantify the impact of human activities in the pollen record. In addition, and for comparison of the M2 pollen record with regional pollen curves, *Juglans* and *Plantago lanceolata* are presented in the OJC and API sums respectively.

3.7. Alkenone-based SST and paleoceanographic/paleoenvironmental indices

Estimates of past sea surface temperature (SST) were calculated on 96 samples by means of the unsaturation ratios of alkenones ($U = C_{37:2}/(C_{37:2} + C_{37:3})$ and the global calibrated parameters of Conte et al. (2006):

$$\left(T = -0.957 + 54.293(U) - 52.894(U)^2 + 28.321(U)^3\right)$$

The analytical precision of our method, based on multi-extractions of sediment samples is better than 0.6 °C. Also, there is an uncertainty associated with the alkenone to SST calibration that, according to Conte et al. (2006) amounts to >1 °C at the 68% confidence level. These values do not represent the full uncertainty associated with the reconstruction and it is worth to note that a quantitative estimation of the uncertainties cannot be achieved within the implemented modeling framework.

In the Aegean Sea, coccosphere fluxes indicate that the main alkenone producer *E. huxleyii* is the dominant species all year round, with higher production and export rates occurring between March and June and secondary maximum from June to November (Triantaphyllou et al., 2004; Malinverno et al., 2009). Therefore, the estimated alkenone patterns and consequently the reconstructed alkenone SSTs are considered to reflect mean annual temperature values. Alkenone unsaturation index measurements calculated using the Conte et al. (2006) equation provide an average of 18.8 °C in the M2 core top (i.e. the ^{210}Pb range, when chronological uncertainties are less than 20 years) and this value shows a good

match with the average historical annual SSTs data (18.2 °C from January 1866 to December 2014; Kaplan SST V2, Kaplan et al., 1998; Bottomley et al., 1990; Reynolds and Smith, 1994; Parker et al., 1995).

The ratio between *F. profunda* (F) and *E. huxleyi* (E) abundances

$$S = F/F + E$$

is applied as stratification S-index of the upper water column (Triantaphyllou et al., 2009b; 2014; Triantaphyllou, 2014). High values in the S-index (values closer to 1) indicate relatively deep nutricline/thermocline position, while low values (values closer to 0) imply high paleoproductivity (sensu Flores et al., 2000).

Grelaud et al. (2012) have shown an exponential anticorrelation between *F. profunda* percentages and surface water Chl-a concentrations throughout the eastern Mediterranean, in agreement with previous studies (Beaufort et al., 2001; Incarbona et al., 2008). Subsequently, the increase of *F. profunda* relative abundance is associated with decline of primary productivity of the surface waters, which shifts to the deeper layers of the water column. Thus, *F. profunda* percentage is used as productivity index in the present study, following Grelaud et al. (2012).

The relation of the abundances of long chain n-alkanes and n-alkanols (HPA Index; Poynter and Eglinton, 1990)

$$HPA = TerN - OH/(TerNA + TerN - OH)$$

is used to evaluate the proportions of labile and refractory organic matter delivered in the marine environment, as also as the *in situ* preservation vs. degradation trends under different redox conditions.

The sum of fresh water palynomorphs (*Pseudoschizaea, Pediastrum* spp., Zygnemantaceae) and soil habitats arbuscular mycorrhizal fungi (Van Geel et al., 1989; Kołaczek et al., 2013) has been used to describe fluctuations of fluvial discharge in the marine environment.

Finally, the pollen ratio

H = AP/St (AP: Arboreal taxa excluding Pinus; St: Artemisia, Chenopodiaceae, Asteraceae and Poaceae).

is used as a humidity (H) index (H-index; Triantaphyllou et al., 2009b; Kouli et al., 2012). Even though its value in human disturbed vegetation patterns is questionable, H-index may act additively if used in parallel with other, independent marine proxies.

In order to highlight the long-term behavior and due to the irregular data sampling, a smoothing local adaptive kernel regression (Wand and Jones, 1995; Herrmann, 1997) is applied to all indices used in this study as well as to the reconstructed SST. The selection of the local bandwidths for the kernel regression is driven by the estimated age-dating uncertainties. Furthermore, to take into account the age-uncertainties of the reconstructed SSTs, an 1000-member ensemble of smoothed-reconstructed SSTs is derived by using a Monte-Carlo approach based on the estimated standard deviations of the age-dating procedures. It is important to underline that the ensemble does not contain and show the full uncertainties of the reconstruction process that cannot be, in the current modeling framework, estimated.

4. Results

4.1. TOC and $\delta^{13}C_{org}$

The vertical profile of the OC contents and $\delta^{13}C$ values is shown in Fig. 4. OC contents range from 0.52 to 1.25%, averaging 0.77 ± 0.14%, with their distribution being marked by periods of increasing and decreasing values. An increasing trend is observed between ca. 500 and 900 AD, followed by pulses of enhanced values between 900 and 1500 AD. Subsequently, the values show an increasing trend until present.

$\delta^{13}C$ values range between −26.1 and −21.6‰. Relatively depleted values are observed between ca. 500 and 900 AD, followed by increased average values and pulses of less depleted signatures between ca. 900 and 1650 AD. Afterwards, the values show an increasing trend and a stabilization around ~23‰ from ca. 1850 AD until present.

4.2. Lipid biomarkers

Abundances of lipid biomarkers are presented in Fig. 4. As OC can vary due to the supply of inorganic material (dilution effect) the concentrations of the reported lipid compounds are normalized to OC contents.

TerNA ranges from 19.5 to 127 μg g^{-1} OC, 55.7 ± 19.2 μg g^{-1} OC on average, while TerN-OH ranges from 9.18 to 66.2 μg g^{-1} OC, averaging 30.4 ± 12.8 μg g^{-1} OC. TerNA and TerN-OH show similar fluctuations with a decreasing trend recorded from ca. 550 to 1000 AD, followed by slightly increased terrestrial inputs between ca. 1000 and 1250 AD and a subsequent decrease until ca. 1400 AD, where minimum values for both TerNA and TerN-OH are recorded. Thereafter, an increasing trend with marked periods of oscillations for TerNA and TerN-OH concentrations is evident until present.

∑Algal ranged between 5.3 and 53 μg g^{-1} OC (av. 20.5 ± 11.6 μg g^{-1} OC). A decreasing trend for the sum of algal biomarkers is observed from ca. 550 to 1400 AD, where minimum values are recorded, with marked periods of oscillations and three distinct peaks around ca. 550 AD, 850 AD and 1200 AD. Subsequently, a general increasing trend is observed for ∑Algal until ca. 1800 AD, with peaks around ca. 1550 AD and 1700 AD. After a sharp decline around ca. 1830 AD, values show a rising trend until present.

CPI_{NA} values range from 4.7 to 9.4 (av. 7.0 ± 0.9), while $CPI_{N\text{-}OH}$ ranges from 5.9 to 9.2, averaging 7.0 ± 0.7, for the whole sedimentary record. These values are consistent with a terrestrial origin from land plants for these compounds (Ohkouchi et al., 1997). CPI_{NA} and $CPI_{N\text{-}OH}$ values show similar trends with minimum fluctuations observed between 550 and ca. 1850 AD (av. of 7.4 ± 0.5 and 6.8 ± 0.5 for CPI_{NA} and $CPI_{N\text{-}OH}$, respectively), while distinct trends and increased fluctuations are observed from ca. 1850 AD to present, where CPI_{NA} values decrease (5.8 ± 0.6) while $CPI_{N\text{-}OH}$ increases (7.6 ± 0.7) from the average values, respectively.

4.3. Coccolithophores

In the period 600–1450 AD *E. huxleyi* abundances remain consistently above 50% (Fig. 5). Afterwards and until present, its relative frequency shows intense fluctuations, to decreased values < 40% between 1450 and 1600 AD; prominent minimum are recorded at 1950 ± 5 AD. *Emiliania huxleyi* reaches approximately 80% during ca. 1050–1100 and 1350–1450 AD, while peaks are also observed at 1650, 1780 and 1987 AD.

An opposite trend is recorded for *F. profunda* (Fig. 5), which presents abundances below 40% up to 1450 AD, whereas it prominently increases (up to 60%) between ca. 1450 and 1600 AD. A sharp decrease of *F. profunda* is recorded at 1650 ± 45 and 1780 ± 18 AD; relatively low (<40%) species values are observed during ca. 1050–1100 AD and 1350–1450 AD. Prominent peaks in abundance (>80%) are observed at 1600 ± 58 and 1950 ± 5 AD; an increasing trend is generally featuring the time interval from ca. 1850 AD until recent times.

Helicosphaera spp. (mainly *H. carteri*) are contributing to the assemblages with very low values, however they start to increase after ca. 1650 AD (Fig. 5). Similar increasing pattern is inferred also for the warm species record. In contrast, *B. bigelowii* fluctuates in

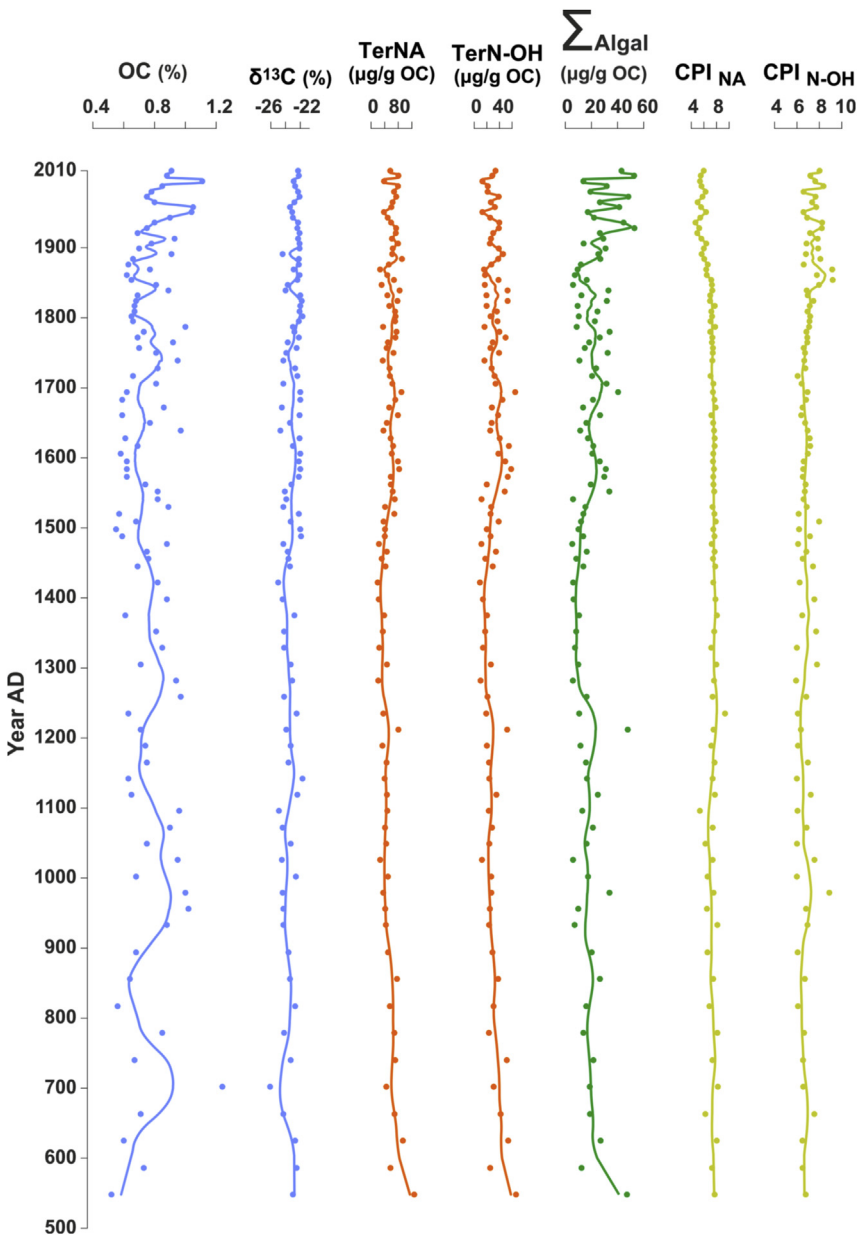

Fig. 4. OC contents, $\delta^{13}C$ values and considered lipid biomarkers' concentrations and indices vs. calibrated age along M2 core. Abbreviations of lipid biomarkers are defined in the text. Bold lines represent the long-term behavior as given by the smoothing local adaptive kernel regression.

abundance from ca. 600 until 1700 AD; afterwards and until present, it is practically absent (Fig. 5).

4.4. Pollen data

Tree taxa are the main species of the sequence but show considerable variations in their abundance (Fig. 6). Forestation cover index (F-Index) exhibits a smooth decreasing trend from 1100 to about 1500 AD, fluctuates sharply in-between 1600 to 1800 AD and increases afterwards to reach its highest level in the mid-20th century. Deciduous forest elements, including deciduous oaks, participate modestly in the pollen flora; increased abundances occur around ca. 1000 to 1200, 1300 to 1500, 1600 to 1750 AD and after 1850 AD. Low values of deciduous *Quercus* are observed around ca. 1250, 1400, 1500 and 1650–1700 AD. Mountainous vegetation appears as sharp short-lived peaks at 1500 ± 51, 1680 ± 37, 1730 ± 25 and 1800 ± 17 AD. Mediterranean elements minima are observed around 1500 AD, in-between ca. 1650 to 1700 AD and around 1800 AD. Furthermore evergreen *Quercus* show another minimum in-between ca. 1350 to 1400 AD. The impact of human activity on vegetation is featured by the curve of API and to smaller extent by the OJC group; the latter being discontinuous. Human impact seems very low around ca. 1050, 1500 and 1800 AD. Fluvial discharge index (Fig. 6), shows highest and highly variable values in between ca. 1550 AD and 1750 AD, while it also increases around 1000 to 1150 AD.

Even though pollen reconstructions have been commonly used to feature the vegetation dynamics in response to climatic fluctuations in the past (including the Holocene period; *e.g.*, Kotthoff et al., 2008; Dormoy et al., 2009; Peyron et al., 2011; 2013), distinguishing between climate and human impacts on vegetation is not possible for the late Holocene (Mercuri and Sadori, 2014), unless historical documentary data are considered (Haldon et al., 2014; Sadori et al., 2015; this study).

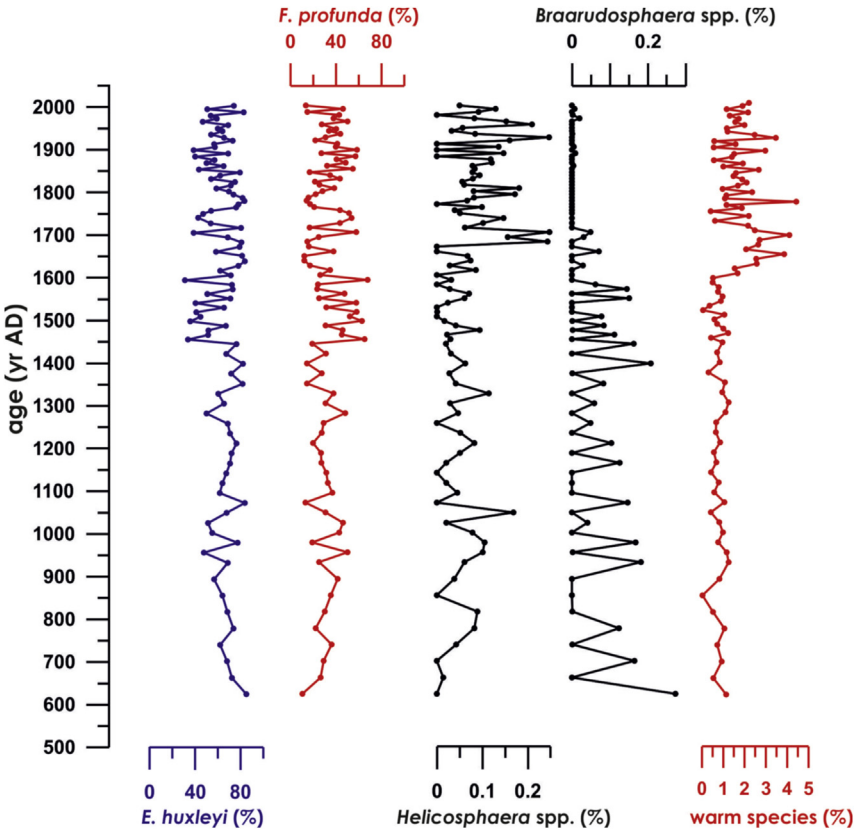

Fig. 5. Relative abundance of coccolithophore species vs. calibrated age along M2 core. Results are expressed in percent (%).

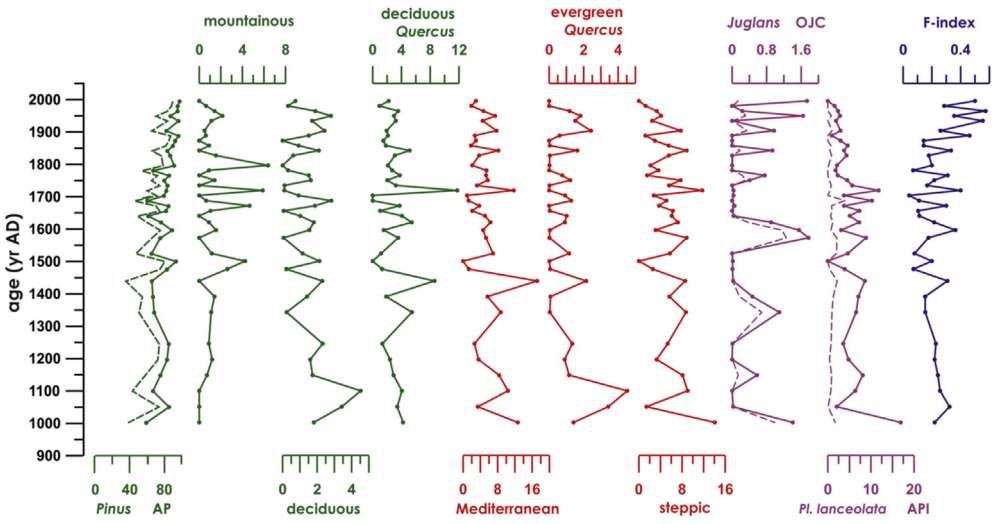

Fig. 6. Abundance curves of the most indicative pollen groups vs. calibrated age along M2 core. Pollen groups are defined in the text. F-index: broadleaved tree versus PS excluding bisaccates ratio (Fluvial discharge Index).

4.5. Alkenone-SST and paleoceanographic/paleoenvironmental indices

The first SST record for the last 1500 years in the north Aegean/NE Mediterranean Sea revealed distinct changes of cool/warm intervals (Fig. 7). The beginning of the reconstructed period shows a drop in the mean SST level around 600 AD, however large uncertainties affect this period as few records are available. In the 8th century and in the first half of the 9th century, the reconstructed SST shows a relatively constant pattern. During the subsequent centuries until the beginning of the 14th century, the reconstructed SST reveals a constant upward trend (synchronous to the MCA period; see Xoplaki et al., 2016) with a large fluctuation around the 10th century. While the 14th and the 15th centuries show steady SSTs, the 16th century is characterized by significant fluctuations. A strong cooling of almost 1.5 °C is observed from the end of the 16th century to the beginning of the 18th century AD. This cooling is followed by a prominent warming until the end of the record,

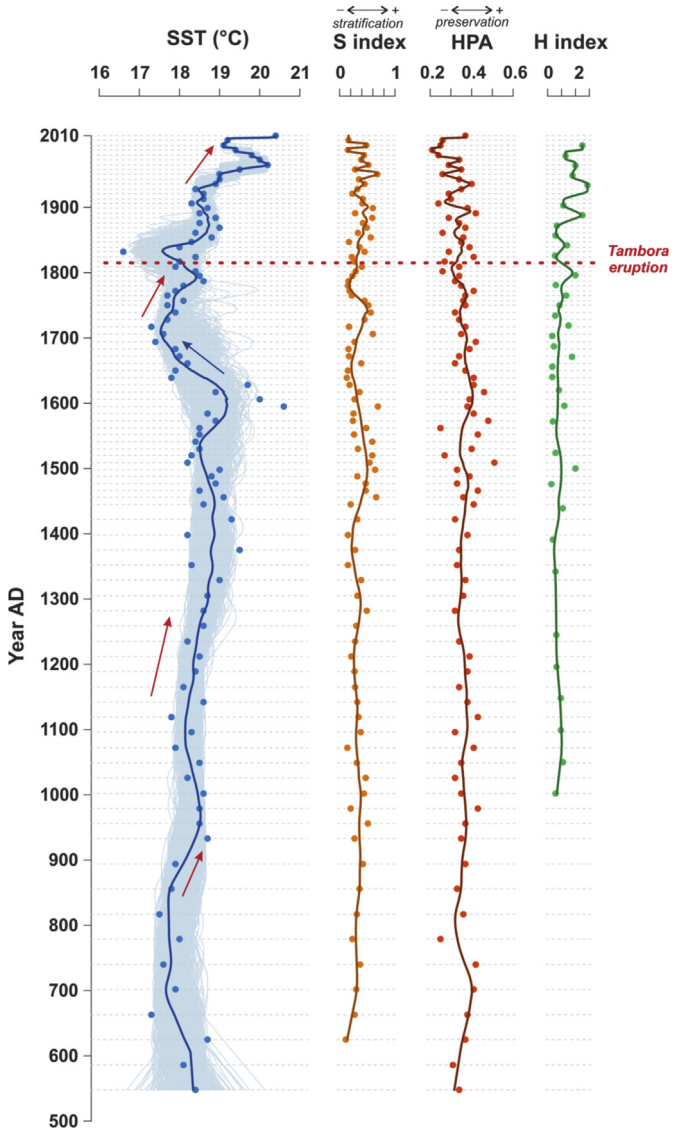

Fig. 7. Reconstructed SSTs (°C), Stratification (S), Higher Plant Alkanol (HPA) and Humidity (H) indices. Bold lines represent the long-term behavior as given by the smoothing local adaptive kernel regression. In the SST panel, the light blue envelop is associated with the 1000-member ensemble. (For interpretation of the references to colour in this figure legend, the reader is referred to the web version of this article.)

interrupted by two main cooling events at 1832 ± 15 AD (16.6 °C) and 1995 ± 1 AD (19.1 °C). Within this period, maximum SSTs of 20.2 and 20.4 °C are recorded at 1965 ± 4 AD and 2010 AD, respectively. Application of an adaptive Kernel smoothing with the local bandwidth given by the uncertainties suggests that the current warming in the reconstructed SSTs of the north Aegean might be unprecedented in the context of the past 1500 years.

Main positive shifts in the water column stratification, as indicated by the stratification S-index, occur at 1450 ± 46 and 1750 ± 21 and since the beginning of the 19th century AD, whereas prominent low values for the index are recorded during the second half of the 18th century AD. The HPA index presents slight fluctuations between ca. 550 and 1450 AD. Maximum fluctuations for this index are observed between ca. 1450 and 1600 AD, followed by slightly decreasing values. Pollen based humidity H-index (Fig. 7) is characterized by a slow but constant increase since ca. 1400 AD, with stronger fluctuation after ca. 1700 AD and presents highest values during the recent 20th century.

5. Discussion

The multidisciplinary approach applied here uses selected marine and terrestrially-derived biogeochemical indices in combination with micropaleontological and palynological evidence retrieved from the M2 sedimentary record and addresses the following research topics: (1) assessment of climate shifts at decadal to multi-decadal temporal resolution for the past 1.5 kyrs in the north Aegean region/NE Mediterranean, (2) identification of land-sea climate interactions and their phase-associations, (3) identification of sensitivities and response-modes to temperature and hydrological changes and (4) assessment of the links between climate and socio-environmental changes in the north Aegean.

5.1. North Aegean climate variability during the last 1500 years based on the M2 proxy-reconstructions

Proxy-reconstructions of the M2 record, reveal an SST cooling trend of almost 1 °C from ca. 500 to 850 AD followed by a warming from ca.850 AD to 950 AD in the northern Aegean (Fig. 7). From ca. 500 to 950 AD, relatively higher concentrations of terrestrial biomarkers (compared to the following period from ca. 950 until 1400 AD; TerNA and TerN-OH; Fig. 4), and depleted $\delta^{13}C$ values, suggest higher supply from continental/riverine runoffs (e.g., Gogou et al., 2007; Triantaphyllou et al., 2009a; 2014). This assumption is supported by slight peaks of *B. bigelowii* and *Helicosphaera* spp. which are most likely related to pulses of fresh water inputs into the basin (Fig. 5; e.g., Negri and Giunta, 2001; Triantaphyllou et al., 2009a; b; Triantaphyllou, 2014). At the same time, low values of *F. profunda* percentages (Fig. 5) indicate elevated *in-situ* productivity, presumably triggered by increases in nutrient availability, which further support the hypothesis of enhanced continental inputs during this time.

From ca. 850 to 950 AD, SSTs at warming are in line with increases of the HPA index (Fig. 7), indicating higher preservation of organic matter due to reduced water column mixing (e.g., Kouli et al., 2012). From ca. 1000–1300 AD, fluctuating SSTs (Fig. 7), together with higher values of *F. profunda* and *B. bigelowii* (Fig. 5), support the establishment of low-salinity stratified waters and the presence of nutrient-rich environment in the deep photic zone (e.g., Molfino and McIntyre, 1990; Triantaphyllou et al., 2009a; Triantaphyllou, 2014).

Strong indications of repeated riverine inputs for about the same period are also evident by pulses in terrestrial biomarkers, enhanced algal productivity, and relatively high $\delta^{13}C$ values (Fig. 4). This is also consistent with palynological data (Fig. 6). The SST fluctuations along with slightly negative shifts in the S- and HPA indices (Figs. 7) and *F. profunda* (Fig. 5) records, possibly respond to water column mixing episodes, associated with cool spells and dense water formation in the north Aegean Sea during this time (e.g., Triantaphyllou, 2014; Triantaphyllou et al., 2016).

A positive trend in SST starts at the end of the 11th century and reachs highest values towards the end of the 16th century. The warm coccolithophore species increase between ca. 1550–1700 AD, supporting high surface water temperatures, whereas rise in both *F. profunda* and the coccolithophore stratification S-index between ca. 1450–1600 AD points to the development of Deep Chlorophyll Maximum (DCM) and intensification of the water column stratification that likely promotes *in-situ* preservation of exported organic matter. Additional evidence to these observations is given by the higher HPA index values, increasing $\delta^{13}C$ values and higher algal biomarkers concentrations (Figs. 4 and 7). Furthermore, a transition from arid-like conditions between ca. 1250–1400 AD towards more humid conditions after ca. 1400 AD is observed, as implied by enhanced supply of land plant inputs (TerNA and TerN-OH; Fig. 4)

and the plant based humidity index (H-index) values (Fig. 7). In the second part of the 17th century and early 18th century, stratification of the upper water column decreases with concomitant productivity increase, as witnessed by lowering of the S-index and rise in ∑Algal and $\delta^{13}C$ values, due probably to enhanced winter mixing conditions, following SST minima (Figs. 4 and 7). The same evolution is observed, marked by an event of rapid SST drop at 1832 ± 15 AD years, possibly related to the 'unknown' volcano eruption in 1809 and the April 1815 Tambora volcanic eruption (Stothers, 1984; Oppenheimer, 2003 see Raible et al. (2016) for a review). The early 18th century is associated with a decrease of *F. profunda* and simultaneous increase of *E. huxleyi* placoliths (Fig. 5), probably linked with the Dalton solar minimum (Wagner and Zorita, 2005; and references therein). Similar findings have been reported by Incarbona et al. (2010) from the Central Mediterranean region.

Periods of rather high stratification in the north Aegean Sea (rises of S-index at ca. 950, 1450 AD), marked also by simultaneous increase in the supply of terrigenous material (TerNA and TerN-OH) and increases of the HPA index, are well correlated with findings from previous studies, highlighting major flood events in the eastern Mediterranean (Luterbacher et al., 2012 and references therein) and indicate wet conditions in the north Aegean Sea region (Figs. 4–7). The concomitant increase of *Helicosphaera* spp. supports the hypothesis of higher fresh water inputs in the core site during these times (e.g., Triantaphyllou et al., 2009a; Triantaphyllou, 2014). Unstable terrestrial hydrologic regime and repeated flooding events are also assumed by the sharp fluctuations of H-index after ca. 1400 AD (Fig. 7), TerNA and TerN-OH concentrations together with shifts in the isotopic signature ($\delta^{13}C$) to relatively depleted values (Fig. 4), as well as the increase of fluvial discharge evidences from pollen data in between ca. 1600 and 1750 AD (Fig.6).

M2 SSTs show a rising trend during the 20th century, accompanied by enhanced terrigenous inputs (TerNA and TerN-OH) of fresh plant material (CPI_{N-OH}) and algal productivity in the euphotic zone (high *F. profunda* percentages; rises of ∑Algal; OC; shift of $\delta^{13}C$ towards higher values), along with prominent increase of warm coccolithophores such as *Rhabdosphaera* spp., *Syracosphaera* spp., *Umbellosphaera* spp. (Figs. 4–7). Decrease in the CPI_{NA} index, along with the gradual development of an 'unresolved complex mixture' of aliphatic hydrocarbons (data not shown), indicate overall enhanced inputs of anthropogenic hydrocarbons deriving from the combustion of coal and fossil fuel products to the study site (Parinos et al., 2013).

5.2. Comparison with other proxy-records from the Mediterranean and the Anatolian regions

Focusing on the hydrological cycle of the Mediterranean during the last 1.1 ky, a synthesis study of continental and marine palaeoclimatic records (Roberts et al., 2012), showed generally drier hydro-climatic conditions during the LIA and a wetter phase during the MCA in the eastern Mediterranean and Anatolian regions. Stalagmite information has been collected in three different regions of Turkey, and several records cover the last 2k years continuously at high resolutions (Fleitmann et al., 2009; Göktürk et al., 2011, Fig. 8). A 2500-year long, seasonally resolved oxygen and carbon isotope record from a stalagmite from Sofular Cave shows a strong correlation with the amount of precipitation and thus effective moisture. Sofular Cave (Fleitmann et al., 2009) shows a long-term decrease in precipitation and effective moisture, but no distinct MCA or LIA. The clearest MCA and LIA pattern has been recorded from a stalagmite in Kocain Cave (southern Turkey), indicating decreased precipitation during the MCA, followed by a wetter LIA (Graham et al., 2011, Fig. 8). In contrast Nar Gölü $\delta^{18}O$ lake record shows wet MCA in respect to drier LIA conditions (Roberts et al., 2012; Dean et al., 2013, Fig. 8). The SSTs peak in the M2 record at ca. 1600 AD, when compared to Sofular, Uzuntarla and particularly Kocain $\delta^{13}C$ records (Fig. 8) is related to wet conditions, supporting the concept of wet LIA in this part of the eastern Mediterranean. This is also expressed in the May-June precipitation in NE Greece and Turkey record of Griggs et al. (2007). Furthermore, the cold shifts at around 1700 AD and mid–19th century in the north Aegean correspond in time with dry conditions in Sofular and Uzuntarla records; interestingly both shifts point to wet periods in the Kocain Cave $\delta^{13}C$ (Fig. 8). We should mention thought that dating uncertainties restrict in many cases the comparison between different archives (e.g. marine, lake and stalagmite records).

Consistency has been observed between records from Anatolia and the Middle East for the period between ca. 800 and 1750 AD, indicating generally wetter climatic conditions around 1200 CE and somewhat drier conditions afterwards (Roberts et al., 2012; Luterbacher et al., 2012), while the M2 core proxy-reconstructions add evidence for enhanced riverine/continental inputs and thus wetter conditions after ca. 1450/1500 AD in the north Aegean region (Fig. 7). A contemporaneous increase in flood frequency and alluvial aggradation recorded in the near-by Drama basin (Lespez, 2003) has been correlated with hydroclimatic changes all over Mediterranean Europe during this period (Camuffo and Enzi, 1996; Grove, 2001). More to the south, evidence from Vravron coastal marsh, Attica, document a marked increase in abundance of Chenopodiaceae and hydrophilous herbs indicating fluvial discharge and the expansion of the wetland (Triantaphyllou et al., 2010; Kouli, 2012). Roberts et al. (2012) have shown that while western Mediterranean aridity/humidity patterns appeared consistent during the MCA/LIA periods, the pattern is less clear in the eastern Mediterranean, implying that the hydroclimatic patterns at various periods and different regions in the Mediterranean were probably determined by a combination of different climate modes along with major physical geographical controls.

Comparison of the M2 north Aegean SST record with the few available Mediterranean marine records (Fig. 2; Alboran Sea, Nieto-Moreno et al., 2013; Gulf of Taranto, Grauel et al., 2013; Balearic Sea, Moreno et al., 2012) suggests that climate signals are not uniform amongst the various basins. Interestingly, the north Aegean M2 record shows recent warming initially starting after 1100 AD and intensified after 1700 AD, which is also recorded in the core from the Gulf of Taranto (Grauel et al., 2013) and in one of the two Alboran sea cores (384B; Nieto-Moreno et al., 2013). Furthermore, the last three century pronounced warming trend observed in our record, is also present in the Central Mediterranean records (Versteegh et al., 2007; Grauel et al., 2013), but it is not apparent in the western Mediterranean records. SST variability in the Mediterranean is mainly controlled by variations in the air–sea heat flux as well as in the vertical mixing, related also to the momentum flux at the air-sea interface and the horizontal advection of heat. Fresh and relatively cold Black Sea waters, entering into the north Aegean through the narrow Dardanelles straits provide an extra term controlling the SSTs distribution and variability in this region (Fig. 2), while the inflow of the fresh Atlantic waters at the surface, taking place at the Gibraltar Strait, represents an additional significant heat source term acting to balance the mean annual net heat loss. Finally, the influence of the prevailing regional and/or large scale atmospheric circulation patterns is another important factor which controls the Mediterranean SST variability (see below, section 5.3.).

5.3. Potential links with large scale climatological patterns

The direct relation of SSTs variability to the climatological parameters at the sea surface through the air-sea heat and

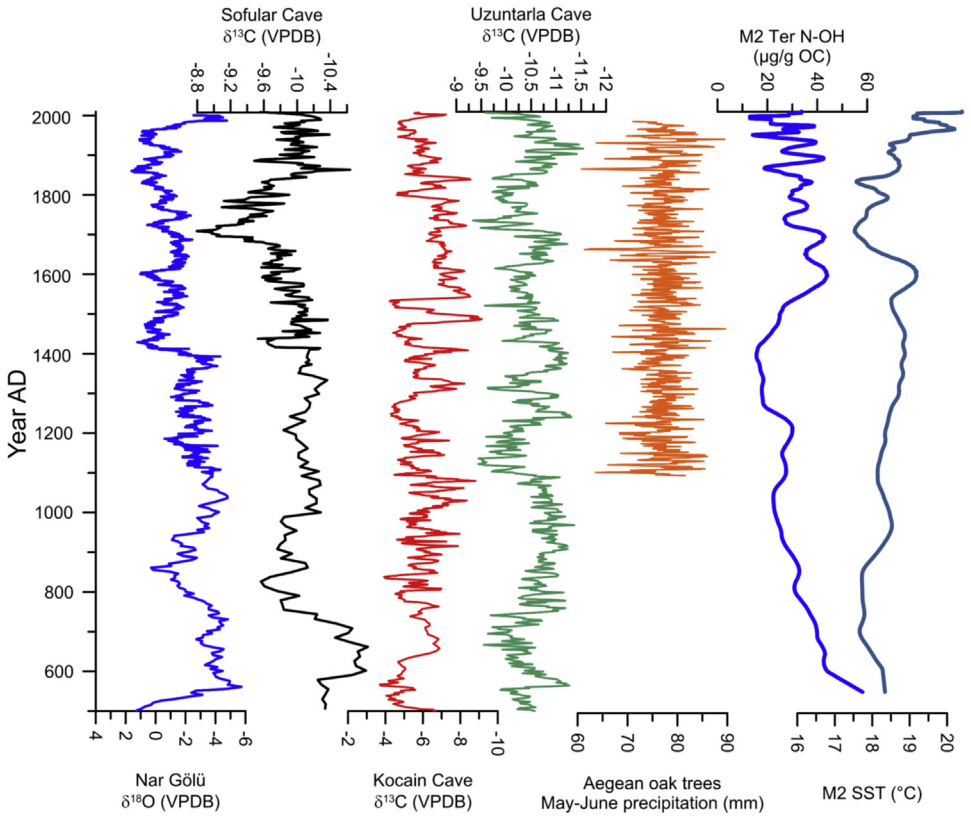

Fig. 8. Comparison of M2 alkenone-SST (°C) and Ter-N-OH (g/g OC; proxy-index for riverine/continental runoffs) with high-resolution stalagmite isotope profiles (oxygen and carbon) from continental sites of the Anatolia region (Fleitmann et al., 2009; Göktürk et al., 2011; Graham et al., Roberts et al., 2012; Dean et al., 2013) and May-June precipitation of Aegean oak trees (Griggs et al., 2007).

momentum fluxes point to the leading patterns of atmospheric variability that influence the climate conditions over the Mediterranean region. The most important large scale mode of climate variability in the Northern Hemisphere with implications to the climate distribution over the Mediterranean Sea is the North Atlantic Oscillation (NAO). NAO is a meridional in atmospheric pressure seesaw pattern between the Icelandic Low and the Azores High (Hurrell et al., 2003). In the Mediterranean Sea, positive winter NAO is connected with relatively warm western Mediterranean and cold eastern Mediterranean Basin (Luterbacher and Xoplaki, 2003), accounting for the surface heat flux dipole structure across the Mediterranean basin (Josey et al., 2011; Papadopoulos et al., 2012). According to these studies, prevailing negative NAO relates with cool SSTs in the NW Mediterranean Sea, and warmer SSTs in the Aegean Sea. This is a result of the prevailing anomalous southerly winds over the eastern Mediterranean, bringing warmer air masses over the area (Hurrell et al., 2003; Kontoyiannis et al., 2012; Skliris et al., 2012). Cold and dry, continental, air advection from northern directions over the Black Sea and the eastern Mediterranean also occurs under high positive East Atlantic/Western Russian (EA/WR) in winter (Kutiel et al., 2002; Josey et al., 2011; Kontoyiannis et al., 2012; Xoplaki et al., 2004). The East Atlantic (EA) pattern is another important atmospheric mode that influences the Mediterranean Sea climate. Interestingly, while NAO results in a dipole structure of heat flux anomalies, with a E-W sign reversal across the Mediterranean (similar to EA/WR), the heat flux anomaly across the whole basin is of the same sign under EA, with positive/negative state producing reduced/enhanced heat loss (Josey et al., 2011).

Teleconnections affecting the Mediterranean climate on multidecadal to centennial time scales, present a large temporal variability and strong seasonal cycles (Ulbrich et al., 2013). Amongst them, the Atlantic Multidecadal Oscillation (AMO) has its principal expression in the SSTs variability of the North Atlantic (Schlesinger, 1994). Mariotti and Dell'Aquila (2012) claimed the existence of a close relationship between AMO and the Mediterranean SSTs at decadal timescales, while Marullo et al. (2011) showed the presence of a significant oscillation of the Mediterranean SSTs with a period of about 70 years, very close to that of the AMO. Skliris et al. (2012) have showed that the recent warming trend in the Mediterranean surface waters is highly correlated with both the Eastern Atlantic (EA) pattern and the Atlantic Multidecadal Oscillation (AMO) index.

In the M2 record, negative SST anomalies during the MCA (ca. 600–1200 AD) coincide with increased frequency of positive AMO events (Fig. 9; Mann et al., 2009), while SST positive anomalies coincide in some cases with negative NAO/AMO states; most prominent the ones around the 1600s (Fig. 9; Gray et al., 2004; Mann et al., 2009; Ortega et al., 2015). According to this, severe winters in the Mediterranean region have been related to negative EA and weaker NAO influence (Josey et al., 2011), while negative NAO and positive low frequency EA conditions could have been responsible for unexpected warm spell in SSTs (e.g. the 1600's; Fig. 9; Moore et al., 2011). Negative winter-NAO and AMO states may also be relevant accounting for the warming of the north Aegean upper waters in the mid-1960s. The subsequent marked cooling in the early 1990s in the Aegean, featuring the Eastern Mediterranean Transient (EMT) episode, may be partly related to NAO and/or EA/WR patterns although the processes involved in the EMT development are still under investigation (Kontoyiannis et al., 2012; Romanski et al., 2012; Gačić et al., 2011; Theocharis et al., 2014; Velaoras et al., 2014).

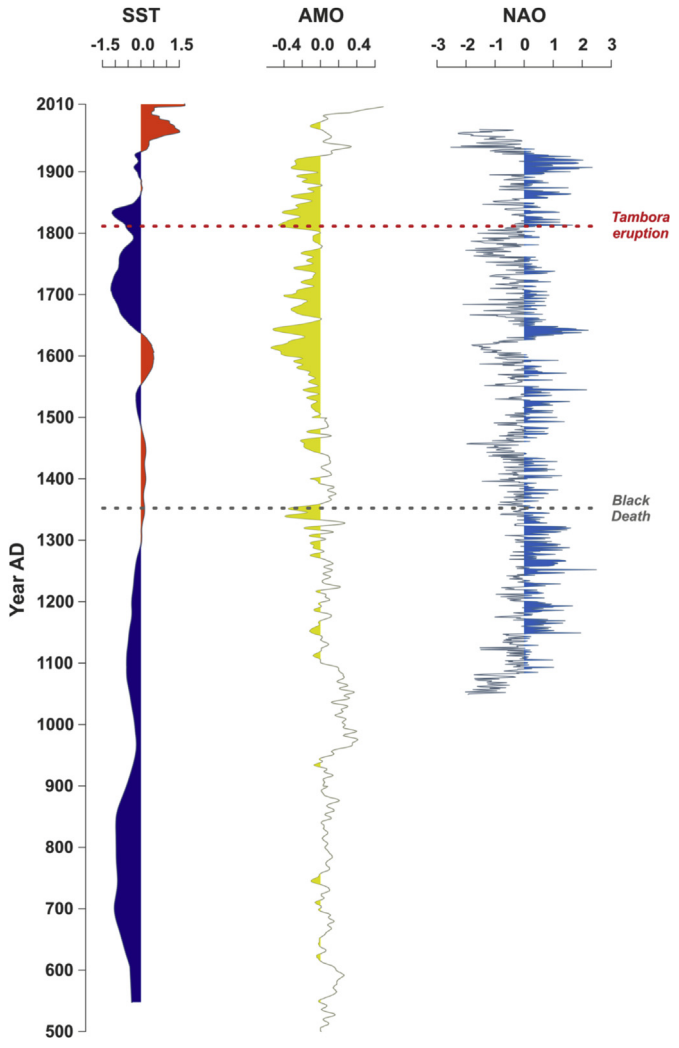

Fig. 9. Left panel: reconstructed mean annual SST in terms of anomalies w.r.t. the 1855–1955 mean. Middle panel: reconstructed AMO index (Mann et al., 2009), shaded green areas show negative AMO periods. Right panel: reconstructed NAO index (Ortega et al., 2015), shaded blue areas show positive NAO periods. (For interpretation of the references to colour in this figure legend, the reader is referred to the web version of this article.)

6. Links between climate and socio-environmental changes in the north Aegean area over the last 1500 years

6.1. Economic expansion during stable/warm climate conditions

During the last 1500 years, until the onset of the modern economic system after 1800 AD, the lands of Macedonia and the Rhodope experienced at least two major cycles of economic and demographic expansion: medieval (culminating in 1200–1350 AD), and early modern (culminating in 1500–1600 AD). In the 5th to 10th centuries, before the period of the medieval growth began, Macedonia was a buffer zone between the Byzantine possessions in the South Balkan littoral and the inimical polities in the northern Balkans, first the Avars and then the Bulgars (Curta, 2006). From ca. 580–600 AD onwards the North Aegean became the focus of considerable Slav migration, which led to a deep transformation of the region's settlement and demographic patterns (Lemerle, 1979; Curta, 2012). During these centuries, as shown by the analysis of the regional pollen data (Fig. 10), both the anthropogenic indicators and the arboreal taxa, the human impact on vegetation in the Macedonian highlands and the Rhodope was not high. This is certainly related to the military and political insecurity which lasted until the conquest of the first Bulgarian Empire by the Byzantines (completed in 1018 AD). Following this event, Macedonia became the central region of the newly-united Byzantine Balkans, which made possible significant economic expansion. However, the first signs of economic growth are visible already prior to that period, with the increase in olive pollen in Macedonia after 800 AD, which certainly has to do with the fact that the reconquest of Southern Macedonia started already after 795 AD and from that period onwards Macedonia became gradually absorbed into the Byzantine market zone. Nevertheless, the major period of growth falls to ca. 1100–1350 AD, as is visible in particular in the cereal pollen data (Fig. 10). As grain products formed the basis of the Byzantine diet (being the source of ca. 50% of the calorie input; Kaplan, 1992, pp. 25–32 and Kokoszko et al., 2014), changes in cereal cultivation can be considered to be related to demographic trends, although this is not a straightforward relation and fluctuations in cereal pollen should not be interpreted as direct proxies for changes in population numbers (Izdebski et al., 2016; see also Fig. 11).

During the Middle Ages, there also occurred some interesting developments in the Rhodope (Fig. 1). An expansion of pastoral indicators is found together with an increase in vine and walnut pollen in the period of ca. 600–1050 AD, with the climax in ca. 1000 AD (Fig. 10). Vine must have grown in the immediate vicinity of the pollen sites, since vine pollen is only transported for short distances (Turner, 2004). This intensification of both vine and walnut cultivation occurred during a period when the average temperature conditions were relatively stable and were increasing steadily, as shown in the M2 SST record (Fig. 7). While a proper assessment of the importance of the climatic factor for the observed pattern of highland agriculture would require a detailed historical study of the entire regional economic and political context, certainly the increase in vine and walnut cultivation was facilitated by the prevalent climatic conditions (if no actually made possible, given the fact that all the available pollen sites in the Rhodope are located on rather high elevations). A decline in vine and walnut pollen occurs after ca. 1000 AD, coinciding with the occurrence of cool spells towards the end of the 11th/beginning of the 12th c., as indicated by M2 SST (Fig. 7). The same seems to be also the case with walnut in the Macedonian highlands, so in more lowland areas, as it shows signs of decline after 1100 AD; olive, in turn, started to decline in Macedonia even prior to that date. To conclude, given the fact that both the olive, walnut and vine cultivation seems to have developed in the North Aegean region during the stable conditions of the 6th to the 11th century, the cool decades of the end of the 11th century might have discouraged further development of these three branches of agricultural production. A similar case of the impact of an episode of very low temperatures (dated to the late 10^{th}-early 11th c.) on the patterns of agricultural production is known from the Iranian Plateau, which specialized in another temperature-sensitive crop, cotton. However, while in the case of Central Asia and Iran the cool spells were one of the factors that contributed to the decline of the previously flourishing Iranian economy and which encouraged the expansion of the pastoral Seljuk Turks (Bulliet, 2009), in Macedonia the cooler decades did not lead to any significant societal change (which at least partly can be explained by the fact that in the end of the 11th c. Macedonia was still relatively loosely populated, cf. Fig. 11).

The economic and demographic expansion in Macedonia, which followed after the political stability was assured in the early 11th c., also occurred during the times of relatively stable climatic conditions, with a warming trend that prevailed throughout the 12th and 13th c. The expansion of agriculture is visible in the increase of cereals (cf. with population dynamics on Fig. 11) and the decrease in

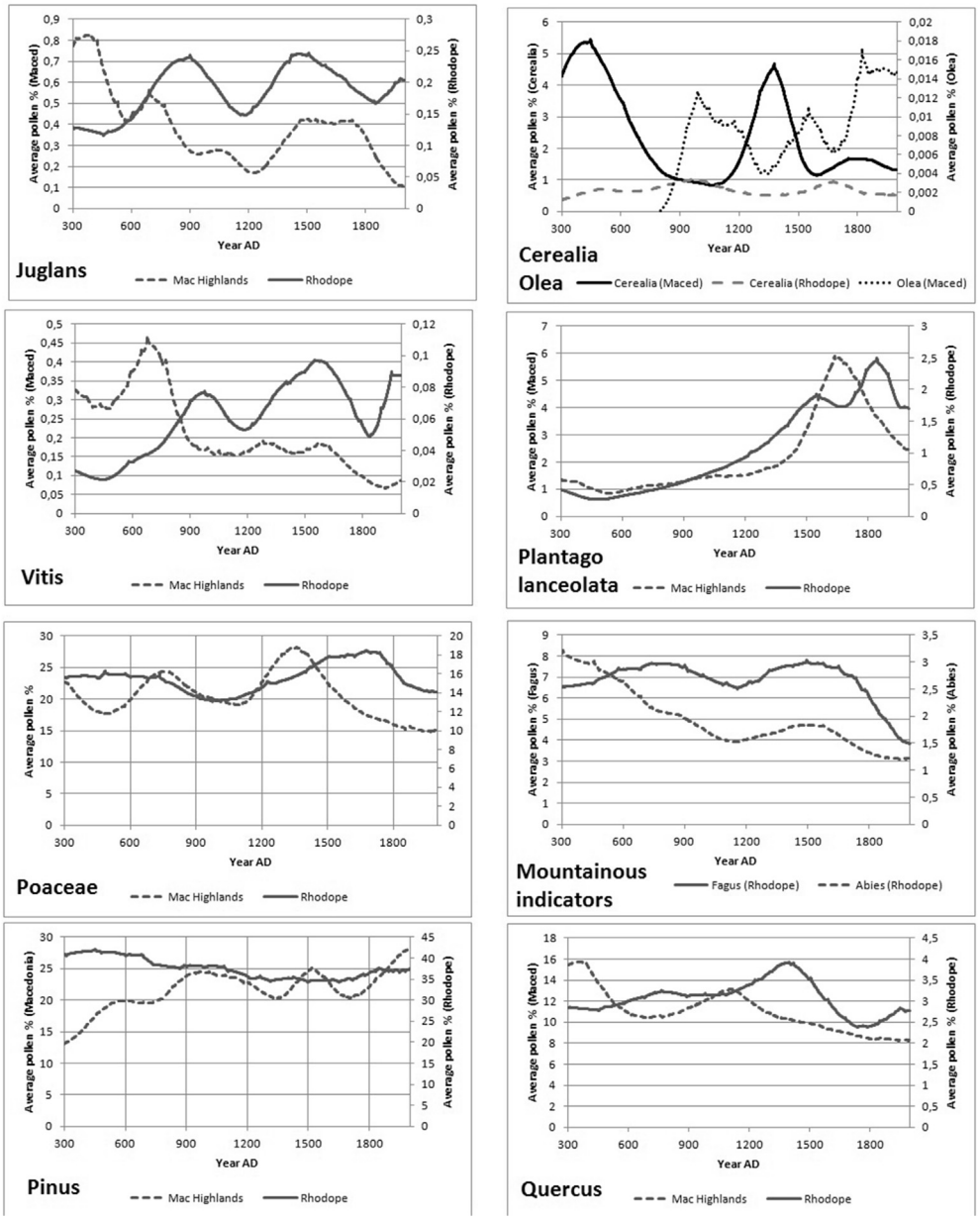

Fig. 10. Regional pollen averages of selected plant taxa for the Macedonian Highlands and the Rhodope. Site locations and regions selected for the analysis are presented in Table 1 and Fig. 1. Source: Izdebski et al., 2015. Data: European Pollen Database.

pine (Fig. 10), as well as in the API record of the marine core M2 (Fig. 6). There also exists considerable textual evidence on the economic growth in Macedonia in the 11th–14th century (Laiou, 1977; Harvey, 1989; Lefort, 1991a; Dunn, 1998). The return of the warming trend did not encourage the restoration of the early medieval patterns in the agricultural economy of the Rhodope, as neither vine nor walnut cultivation increased any more. On the contrary, due to this region's specialization in pastoral activities, the Rhodope increasingly relied on the lowlands for the supply of cultivation products (Izdebski et al., 2015), which actually made its economy less vulnerable to local weather conditions.

In this context, it is worth observing that also the second period of economic expansion corresponds with climatic conditions that certainly facilitated agricultural production. This phase of growth is associated with the prosperity and political stability of the Ottoman Empire's climax in the 16th c. (White, 2011, pp. 20–77), and with the booming trade in grain between the Ottoman lands and the Western Mediterranean (Dunn, 2009; McGowan, 1981, pp. 1–44). Indeed, it was during this period that there occurred more stable climatic conditions with a gradual increase in temperature, while the previous century was characterized by fluctuations between warm and cool events (Fig. 7).

To conclude, at first glance the temporal correlation between the stable climatic conditions, often with a significant warming trend, and phases of economic growth, as visible in agriculture (i.e., pollen indicators) and demography (i.e., Byzantine and Ottoman textual sources), is indeed striking. However, this should not lead to simplistic hypothesis that climate 'amelioration' was responsible for the economic growth; rather, it should encourage further exploration of the causal mechanisms behind the observed phenomena, which would help to understand the role of climate in the proper context. One should remember that neither during the

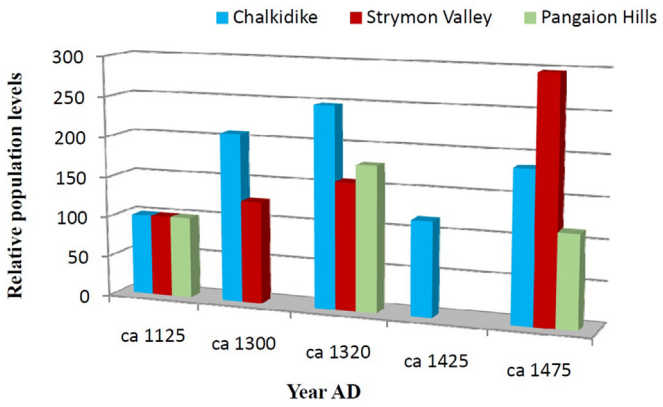

Fig. 11. Relative changes in population numbers in selected sub-regions of Macedonia, as revealed by the Athos archives. Source: (Lefort, 1991b).

Middle Ages nor during the early modern period, climate was the sole factor behind the increase in the scale of human impact on the region's environment. On the contrary, in each case it is possible to point out different societal factors, such as political and military stability, demand for specific products, either on foreign markets or on the part of the state apparatus (in the case of cereals), the possibility to meet local supply needs by imports (in the case of walnut, vine and olive), as main drivers of the observed socio-environmental changes. Nevertheless, it is clear that in particular in the case of the more temperature-sensitive crops the average temperature conditions were crucial for achieving yields that made their cultivation profitable, or at least viable. It is more difficult to establish a clear link between the growth of the medieval or early modern cereal economies in Macedonia and the stable average temperature conditions. This requires, in particular, an exploration of how SST levels translate into weather conditions for cereal cultivation, and what the mechanisms that led to specialization in cereals in the region actually were, whether there were any natural limits to the expansion of cereal farming, which better climate conditions could ameliorate. In this context, it might be particularly interesting to study the response on the part of the cereal economy to the unusually cold and rather unstable conditions of the 17th c., which were completely different from the warm and stable conditions of the 16th c., which saw the growth of the Ottoman cereal cultivation in Macedonia.

6.2. Black Death and its impact on the environment

The Black Death was a recurring problem in Macedonia in the decades that followed after 1348 AD (Dols, 1979; Büntgen et al., 2011; Schmid et al., 2015). Within a relatively short time the plague resulted in considerable population loss, which had damaging effects on the economic trends. The scale of cereal cultivation in the hills surrounding the Macedonian plain declines considerably within the next one to two centuries, which presumably had to do with the dropdown of the population levels. At the same time, the pine pollen increased its share in the pollen signal, which suggests the occurrence of secondary ecological succession onto lands previously used for agricultural activities (Fig. 10). The Byzantine archival data from the Athos monasteries also show considerable population losses. Chalkidike and the Pangaion Hills lost some 30–50% of their inhabitants within some 100 years after the plague first came to Macedonia. Any population decline in the Strymon valley would, however, have been only short-term, as in ca. 1475 the population outnumbered the levels of ca. 1325 AD (Fig. 11; there is no data for the intermediate period).

Geyer (1986, p. 105) suggested that in the hilly parts of Macedonia an episode of increased erosion occurred as a result of this demographic catastrophe. Without human care, abandoned fields located on hills and terraces in river valleys would have quickly lost much of their soils. This hypothesis seems to be confirmed by the pollen-derived fluvial input index of the marine core M2, which shows increased soil erosion in a sample dated to ca. 1375 ± 49 AD. Also other pollen data from the marine core M2 (Fig. 6), show a decline in anthropogenic impact around 1350–1500 AD, and thus it can tentatively be associated with the environmental consequences of the Black Death. Thus, during the first phase of this process, the OJC (olive, walnut, and chestnut) curve decreases to zero values, while the Mediterranean and deciduous vegetation, as well as *Quercus*, increase. This would suggest a decline in agricultural activities and at the same time a secondary succession of wild taxa, when the anthropogenic pressure declined. These developments, however, differ slightly from those observed in the terrestrial pollen record from the Macedonian Highlands, but these lands cannot be considered the source area of the terrestrial components of the marine core M2. Unfortunately, for this period there exists no well-resolved terrestrial pollen data from the lower Strymon valley (which is the primary source area of M2 core), so it is not possible to make a direct comparison of the marine pollen record with any terrestrial pollen data.

6.3. Pastoral activities and mountainous vegetation during the little age

The mountain vegetation is relatively well represented in the marine pollen data. Sharp peaks of mountainous forest taxa in the M2 core are dated ca. 1500 ± 50, 1680 ± 36, 1730 ± 25 and 1800 ± 16 AD (Fig. 6). Given the long history of complex pastoral economy in the Rhodope mountains, these peaks may reflect changes in the patterns of economic activity or climatic fluctuations.

The Byzantine textual sources contain information about large-scale pastoral activities from the 1060s AD (Gyóni, 1951) and in 1180–1200 AD the pastoral Vlachs managed to create the second Bulgarian Empire (Ritter, 2013). Unfortunately, there is no archaeological data and thus it is not possible to reconstruct the development of this highland pastoral economy in the central Balkans (cf. Henning, 1984; 1987). However, the pollen record from the Macedonian Highlands and especially from the Rhodope (Fig. 10) shows a steady increase in *P. lanceolata* (an important indicator of pasturing activities (Behre, 1981)) from 600 AD onwards, as well as the dramatic decrease in *Abies* (fir) and the increase of Poaceae (true grasses), which suggest continued land-opening in the same period; stabilization in fir forest is evident in the regional pollen data after ca. 1000 AD (Fig. 10). The textual sources make it clear that this medieval pastoral economy continued in the later Middle Ages (Popović, 2012) and judging from the *Plantago* curves it must have expanded even further in 1400–1500/1600 AD and again in 1700–1800 AD. These early modern expansion phases may have had to do with the migration of Turcoman nomads into the Rhodope after 1500 AD (Raduschev, 2005) (for a detailed analysis of the Macedonia-Rhodope pastoral economy during the last two thousand years, see Izdebski et al., 2015).

Unfortunately, neither the regional pollen data (the temporal resolution of which is ca. 100 years), nor the historical documents make it possible to get beyond general trends and reconstruct decadal-scale changes, while these might have led to the increased deposition of the pollen produced by the mountain vegetation in the North Aegean Sea. It is conceivable that the earliest peak (ca. 1500) had to do with the longer-term impact of the Black Death and the general worsening of the economic situation in the North Aegean (some pastures would have been abandoned and mountain

trees would grow again). The late 17th and 18th c. peaks (at ca. 1680, 1730, and 1800) fall into the *Fagus* (beech; as well as fir) stabilization and decline recorded in the regional pollen data in-between 1650–1900 AD. They are thus more difficult to interpret in terms of purely anthropogenic causes. Rather, since they are corresponding in time with cooler intervals in the SST record, they seem to have been primarily climate-driven, even if these medium-term cooling phases were mediated by human activities, as herders might have limited their use of high mountain pastures due to the more severe winters and cooler summers.

7. Conclusions

Our paleoclimatic study for the last 1500 years in the northern Aegean, based on multi-proxy reconstructions from the M2 high resolution marine multi-core along with a socio-environmental analysis focused on important periods/events in the same region, concludes as follows: The period from ca. 500 to 900 AD is featured by relatively stable SSTs and a tendency towards higher precipitation and thus increased supply from continental/riverine runoffs. From ca. 1100 AD to 1300 AD, SSTs show an increasing trend and independent multi-proxy evidence from biomarker, marine microfossil and pollen indices, indicate a transition from arid-like conditions towards more humid conditions. After 1600 AD, SSTs exhibit a marked drop, stratification S-index decreases and marine productivity increases, probably due to enhanced winter mixing conditions following SST minima. The 19th century is marked by a strong cooling event at 1832 ± 15 AD, possibly related to the 'unknown' volcano eruption in 1809 and the April 1815 Tambora eruption. The last 100 years of instrumental SST data are characterized by rising SSTs, accompanied by enhanced terrigenous inputs.

Intensified riverine/continental runoffs after ca. 1450 AD in the north Aegean record, suggest humidity increase within the LIA and drier conditions during the MCA. The SST peak at ca. 1600 AD is related to wet conditions, supporting the concept of wet LIA in this part of the eastern Mediterranean. When compared to other eastern Mediterranean and Anatolian continental records, we observe both similarities and differences in the hydroclimatic patterns. This is in agreement with recent findings by Roberts et al. (2012) and Cook et al. (2016), proposing that hydroclimatic patterns at various periods and different regions in the Mediterranean have been probably determined by a combination of different climate modes along with major physical geographical controls. Furthermore, periods of rather increased stratification in the north Aegean Sea (rise of the HPA and S- indices at ca. 950, 1150, 1450, 1600 AD), marked also by simultaneous increase in the supply of terrigenous material, highlight major flood events in the north Aegean, in line with reports from previous studies in the eastern Mediterranean.

Potential links between the paleoclimatic and paleoenvironmental information, as revealed by the comparison of the proxy-based climate reconstructions of the north Aegean marine record with regional and large scale climatological patterns, were investigated. Negative NAO/AMO and positive low frequency EA conditions might have been of importance for the unexpected warm spell around 1600 AD and in mid-1960s in the north Aegean Sea SST record. However, no direct linear relationship can be inferred from the analysis performed in this study, and further in-depth investigation is needed.

The combination of the north Aegean paleoclimatic and and paleoenvironmental proxy-reconstructions with the socio-economic history of Macedonia and the Rhodope has highlighted three important points: a) the comparison of the longer-term patterns of demographic-economic growth (and decline) with the climatic variability showed that fluctuations in temperature are correlated with the development and decline of vine, olive and walnut cultivation in the Macedonian highlands and the Rhodope regions. Moreover, we observed significant temporal correlation between periods of economic (agricultural and demographic) growth and stable warming climate conditions; however, establishing causal links between climate and economy requires further research, focused directly on the issues in question. b) the environmental impact of the Black Death, which struck the region after 1348 AD, seems to have caused a major environmental change in the north Aegean region, which was recorded in the M2 proxy-reconstructions, and c) special attention was given to the development of the pastoral activities in the mountains of the wider North Aegean region, in order to distinguish between the anthropogenic and climatic controls of mountainous vegetation in the marine pollen record. Our findings suggest that the early modern peaks in mountain vegetation visible in the M2 north Aegean core were primarily climate-driven, while in the medieval period a major factor that brought about the transformation of the Rhodope landscapes was the development of the Vlach pastoral economy.

Acknowledgements

This paper emerges as a result from a workshop at the Navarino Environmental Observatory (NEO), Greece in April 2014, addressing Mediterranean Holocene climate and human societies. The workshop was co-sponsored by PAGES, NEO, the MISTRALS/PaleoMex program, the Labex OT-Med, the Bolin Centre for Climate Research at Stockholm University, and the Institute of Oceanography at the Hellenic Centre for Marine Research. Funding was provided by the Greek National Project KRIPIS (Integrated Observatories in the Greek Seas - IO, HCMR-MIS 451724; NSRF), the University of Athens Research Project KA 70/4/11078, and the European Research Projects 'MedEcos' (MarinERA, EU/FP6) and 'Sea for Society' (EU/FP7, Science and Society - 2011-1, 289066). A.I. acknowledges the funding of the National Science Centre, Poland, through its post-doctoral fellowships scheme (DEC-2012/04/S/HS3/00226). B.M. wishes to express her thanks to the CSIC-Ramón y Cajal RYC-2013-14073 post-doctoral programme and the Shackleton Fellowship, Clare Hall, Cambridge. We sincerely thank the officers and crew of *R/V* Aegaeo (HCMR, Greece) for their precious help during the "MEDECOS II" cruise. We would like also to deeply thank two anonymous reviewers for their constructive comments that helped us significantly improve the quality of the manuscript during the revision process.

We dedicate this article to the memory of our colleagues ***Kostas Nittis*** and ***James Casford***. They have inspired us and will continue to inspire future generations with their generosity, dedication and outstanding scientific integrity.

References

Androulidakis, Y.S., Kourafalou, V.H., Krestenitis, Y.N., Zervakis, V., 2012. Variability of deep water mass characteristics in the North Aegean Sea: the role of lateral inputs and atmospheric conditions. Deep-Sea Res. Part I Oceanogr. Res. Pap. 67, 55–72.

Appleby, P.G., Oldfield, F., 1978. The calculation of lead-210 dates assuming a constant rate of supply of unsupported 210Pb to the sediment. Catena 5, 1–8.

Beaufort, L., De Garidel-Thoron, T., Mix, A.C., Pisias, N.G., 2001. ENSO-like forcing on oceanic primary production during the late pleistocene. Science 293, 2440–2444.

Behre, K.-E., 1981. The interpretation of anthropogenic indicators in pollen diagrams. Pollen spores 23, 225–245.

Berger, J.F., Delhon, C., Magnin, F., Bont, S., Peyric, D., Thiebault, S., Guilbert, R., Beeching, A., 2016. A fluvial record of the mid-Holocene rapid climatic changes in the middle Rhone valley (Espeluche-Lalo, France) and of their impact on Late Mesolithic and Early Neolithic societies. Quaternary Science Reviews 136. http://dx.doi.org/10.1016/j.quascirev.2015.11.019 this issue.

Borrell, F., Junno, A., Barceló, J.A., 2015. Synchronous environmental and cultural change in the emergence of agricultural economies 10,000 years ago in the Levant.

PLoS ONE 10 (8), e0134810. http://dx.doi.org/10.1371/journal.pone.0134810.
Bottomley, M., Folland, C.K., Hsiung, J., Newell, R.E., Parker, D.E., 1990. Global Ocean Surface Temperature Atlas.
Brönnimann, S., Xoplaki, E., Casty, C., Pauling, A., Luterbacher, J., 2007. ENSO influence on Europe during the last centuries. Clim. Dyn. 28, 181–197.
Bulliet, R.W., 2009. Cotton, Climate, and Camels in Early Islamic Iran: a Moment in World History. Columbia University Press, New York; Chichester.
Büntgen, U., Tegel, W., Nicolussi, K., McCormick, M., Frank, D., Trouet, V., Kaplan, J.O., Herzig, F., Heussner, K.U., Wanner, H., Luterbacher, J., Esper, J., 2011. 2500 years of European climate variability and human susceptibility. Science 331, 578–582.
Büntgen, U., Trnka, M., Krusic, P.J., Kyncl, T., Kyncl, J., Nicolussi, K., Luterbacher, J., Zorita, E., Ljungqvist, C.F., Auer, I., Konter, O., Schneider, L., Tegel, W., Stepanek, P., Brönnimann, S., Hellmann, L., Nievergelt, D., Esper, J., 2015. Tree-ring amplification of the Early-19th Century summer cooling in Central Europe. J. Clim. 28, 5272–5288.
Camuffo, D., Enzi, S., 1996. he analysis of two bi-millenian series: tiber and Po river floods. In: Jones, P.D., Bradley, R.S., Jouzel, J. (Eds.), Climatic Variations and Forcing Mechanisms of the Last 2000 Years, NATO ASI Series, vol. I (41). Springer, Berlin, pp. 433–450.
Castradori, D., 1993. Calcareous nannofossils and the origin of eastern Mediterranean sapropels. Paleoceanography 8, 459–471.
Conte, M.H., Sicre, M.A., Rühlemann, C., Weber, J.C., Schulte, S., Schulz-Bull, D., Blanz, T., 2006. Global temperature calibration of the alkenone unsaturation index (U 37 k) in surface waters and comparison with surface sediments. Geochem. Geophys. Geosystems 7.
Cook, E.R., Seager, R., Kushnir, Y., Briffa, K.R., Büntgen, U., Frank, D., Krusic, P.J., Tegel, W., van der Schrier, G., Andreu-Hayles, L., Baillie, M., Baittinger, C., Bleicher, N., Bonde, N., Brown, D., Carrer, M., Cooper, R., Cufar, K., Dittmar, C., Esper, J., Griggs, C., Gunnarson, B., Günther, B., Gutierrez, E., Haneca, K., Helama, S., Herzig, F., Heussner, K.-U., Hofmann, J., Janda, P., Kontic, R., Kose, N., Kyncl, T., Levanic, T., Linderholm, H., Manning, S., Melvin, T.M., Miles, D., Neuwirth, B., Nicolussi, K., Nola, P., Panayotov, M., Popa, I., Rothe, A., Seftigen, K., Seim, A., Svarva, H., Svoboda, M., Thun, T., Timonen, M., Touchan, R., Trotsiuk, V., Trouet, V., Walder, F., Wazny, T., Wilson, R., Zang, C., 2015. Old World megadroughts and pluvials during the Common Era. Science Advances 1 (10). http://dx.doi.org/10.1126/sciadv.1500561.
Cook, B.I., Anchukaitis, K.J., Touchan, R., Meko, D.M., Cook, E.R., 2016. Spatiotemporal drought variability in the Mediterranean over the last 900 years. J. Geophys. Res. revised.
Corte-Real, J., Xuebin, Z., Xiaolan, W., 1995. Large-scale circulation regimes and surface climatic anomalies over the Mediterranean. Int. J. Climatol. 15, 1135–1150.
Curta, F., 2006. Southeastern Europe in the Middle Ages, 500–1250. Cambridge University Press, Cambridge.
Curta, F., 2012. Were there any Slavs in seventh-century Macedonia? J. Hist. 47, 61–74.
Dean, J.R., Jones, M.D., Leng, M.J., Sloane, H.J., Roberts, C.N., Woodbridge, J., Swann, G.E.A., Metcalfe, S.E., Eastwood, W.J., Yiğitbaşıoğlu, H., 2013. Palaeoseasonality of the last two millennia reconstructed from the oxygen isotope composition of carbonates and diatom silica from Nar Gölü, central Turkey. Quat. Sci. Rev. 66, 35–44.
deMenocal, P.B., 2001. Cultural responses to climate change during the late Holocene. Science 292, 667–673.
Dimiza, M.D., Triantaphyllou, M.V., Dermitzakis, M.D., 2008. Seasonality and ecology of living coccolithophores in Eastern Mediterranean coastal environments (Andros Island, Middle Aegean Sea). Micropaleontology 54, 159–175.
Dimiza, M.D., Triantaphyllou, M.V., Malinverno, E., Psarra, S., Karatsolis, B., Mara, P., Lalaria, Gogou, A., 2015. The composition and distribution of living coccolithophores in the Aegean Sea (NE Mediterranean). Micropaleontology 61, 524–545.
Dols, M.W., 1979. The second plague pandemic and its recurrences in the middle east: 1347–1894. J. Econ. Soc. Hist. Orient 22, 162–189.
Dormoy, I., Peyron, O., Nebout, N.C., Goring, S., Kotthoff, U., Magny, M., Pross, J., 2009. Terrestrial climate variability and seasonality changes in the Mediterranean region between 15000 and 4000 years BP deduced from marine pollen records. Clim. Past. 5, 615–632.
Dunn, A., 1994. The transition from polis to kastron in the Balkans (III-VII c.), general and regional perspectives. Byzantine Mod. Greek Stud. 18, 60–80.
Dunn, A., 1998. Loci of maritime traffic in the Strymon Delta iv -xviii cc.: commercial, fiscal, manorial. In: Oi Serres Kai I Periokhi Tous Apo Tin Arkhaiotita Stin Metavyzantini Koinonia. Demos Serron, Serres, pp. 339–360.
Dunn, A., 2005. The problem of the early Byzantine village in eastern and northern Macedonia. In: Lefort, J., Morrisson, C., Sodini, J.-P. (Eds.), Les Villages Dans L'empire Byzantin: IVe-XVe Siècle, Réalités Byzantines. Lethielleux, Paris, pp. 267–278.
Dunn, A., 2009. Byzantine and Ottoman maritime traffic in the estuary of the Strymon: between environment, state, and market. In: Bintliff, J., Stöger, H. (Eds.), Medieval and Post-Medieval Greece. The Corfu Papers, BAR International Series. Archaeopress, Oxford.
Eglinton, G., Hamilton, R.J., 1967. Leaf epicuticular waxes. Science 156, 1322–1335.
Eglinton, T.I., Eglinton, G., 2008. Molecular proxies for paleoclimatology. Earth Planet Sci. Lett. 275, 1–16.
Esper, J., Frank, D., Büntgen, U., Verstege, A., Luterbacher, J., Xoplaki, E., 2007. Long-term drought severity variations in Morocco. Geophys. Res. Lett. 34.
Esper, J., Schneider, L., Krusic, P.J., Luterbacher, J., Büntgen, U., Timonen, M., Sirocko, F., Zorita, E., 2013. European summer temperature response to annually dated volcanic eruptions over the past nine centuries. Bull. Volcanol. 75, 1–14.
Fichaut, M., Garcia, M.J., Giorgetti, A., Iona, A., Kuznetsov, A., Rixen, M., Group, M., 2003. MEDAR/MEDATLAS 2002: a Mediterranean and Black Sea database for operational oceanography. In: Dahlin, H., N.C.F.K.N., Petersson, S.E. (Eds.), Elsevier Oceanography Series. Elsevier, pp. 645–648.
Fischer, E.A., Luterbacher, J., Zorita, E., Tett, S.F.B., Casty, C., Wanner, H., 2007. European climate response to tropical volcanic eruptions over the last half millennium. Geophys. Res. Lett. 34.
Fleitmann, D., Cheng, H., Badertscher, S., Edwards, R.L., Mudelsee, M., Göktürk, O.M., Fankhauser, A., Pickering, R., Raible, C.C., Matter, A., Kramers, J., Tüysüz, O., 2009. Timing and climatic impact of Greenland interstadials recorded in stalagmites from northern Turkey. Geophys. Res. Lett. 36.
Flores, J.A., Bárcena, M.A., Sierro, F.J., 2000. Ocean-surface and wind dynamics in the Atlantic Ocean off Northwest Africa during the last 140 000 years. Palaeogeogr. Palaeoclimatol. Palaeoecol. 161, 459–478.
Flores, J.A., Sierro, F.J., Francés, G., Vázquez, A., Zamarreno, I., 1997. The last 100,000 years in the western Mediterranean: sea surface water and frontal dynamics as revealed by coccolithophores. Mar. Micropaleontol. 29, 351–366.
Gačić, M., Civitarese, G., Eusebi Borzelli, G.L., Kovačević, V., Poulain, P.M., Theocharis, A., Menna, M., Catucci, A., Zarokanellos, N., 2011. On the relationship between the decadal oscillations of the northern Ionian Sea and the salinity distributions in the eastern Mediterranean. J. Geophys. Res. C Oceans 116.
Gertman, I., Pinardi, N., Popov, Y., Hecht, A., 2006. Aegean sea water masses during the early stages of the Eastern Mediterranean Climatic Transient (1988–90). J. Phys. Oceanogr. 36, 1841–1859.
Geyer, B., 1986. Esquisse pour une histoire du paysage depuis l'An Mil. In: Lefort, J. (Ed.), Paysages de Macédoine: leurs caractères, leur évolution à travers les documents et les récits des voyageurs. De Boccard, Paris, pp. 99–116.
Gogou, A., Bouloubassi, I., Lykousis, V., Arnaboldi, M., Gaitani, P., Meyers, P.A., 2007. Organic geochemical evidence of Late Glacial-Holocene climate instability in the North Aegean Sea. Palaeogeogr. Palaeoclimatol. Palaeoecol. 256, 1–20.
Göktürk, O.M., Fleitmann, D., Badertscher, S., Cheng, H., Edwards, R.L., Leuenberger, M., Fankhauser, A., Tüysüz, O., Kramers, J., 2011. Climate on the southern Black Sea coast during the Holocene: Implications from the Sofular Cave record. Quat. Sci. Rev. 30, 2433–2445.
Graham, N.E., Ammann, C.M., Fleitmann, D., Cobb, K.M., Luterbacher, J., 2011. Support for global climate reorganization during the "Medieval Climate Anomaly. Clim. Dyn. 37, 1217–1245.
Grauel, A.L., Leider, A., Goudeau, M.L.S., Müller, I.A., Bernasconi, S.M., Hinrichs, K.U., de Lange, G.J., Zonneveld, K.A.F., Versteegh, G.J.M., 2013. What do SST proxies really tell us? A high-resolution multiproxy (UK' 37, TEXH 86 and foraminifera δ18O) study in the Gulf of Taranto, central Mediterranean Sea. Quat. Sci. Rev. 73, 115–131.
Gray, S.T., Graumlich, L.J., Betancourt, J.L., Pederson, G.T., 2004. A tree-ring based reconstruction of the Atlantic Multidecadal oscillation since 1567 A.D. Geophys. Res. Lett. 31, 12201–12204. L12205.
Grelaud, M., Marino, G., Ziveri, P., Rohling, E.J., 2012. Abrupt shoaling of the nutricline in response to massive freshwater flooding at the onset of the last interglacial sapropel event. Paleoceanography 27, PA3208. http://dx.doi.org/10.1029/2012PA002288.
Griggs, C., DeGaetano, A., Kuniholm, P., Newton, M., 2007. A regional high-frequency reconstruction of May-June precipitation in the north Aegean from oak tree rings, A.D. 1089–1989. Int. J. Climatol. 27, 1075–1089.
Grove, A.T., 2001. The "Little ice age" and its geomorphological consequences in Mediterranean Europe. Clim. Change 48, 121–136.
Gyóni, M., 1951. La transhumance des Vlaques balkaniques au Moyen Age. Byzantinoslavica 12, 29–42.
Haldon, J., Roberts, N., Izdebski, A., Fleitmann, D., McCormick, M., Cassis, M., Doonan, O., Eastwood, W., Elton, H., Ladstäter, S., Manning, S., Newhard, J., Nichol, K., Telelis, I., Xoplaki, E., 2014. The climate and environment of Byzantine Anatolia: integrating science, history and archaeology. J. Interdiscip. Hist. 45, 113–161.
Harvey, A., 1989. Economic Expansion in the Byzantine Empire, 900–1200. Cambridge University Press, Cambridge.
Henning, J., 1984. Untersuchungen zur Entwicklung der Landwirtschaft in Südosteuropa im Übergang von der Spätantike zum frühen Mittelalter. Ethnogr. Z. 25, 123–130.
Henning, J., 1987. Südosteuropa zwischen Antike und Mittelalter, Schriften zur Ur- und Frühgeschichte. Akademie-Verlag, Berlin.
Herrmann, E., 1997. Local bandwidth choice in kernel regression estimation. J. Comput. Graph. Statistics 6, 35–54.
Hinrichs, K.U., Schneider, R.R., Müller, P.J., Rullkötter, J., 1999. A biomarker perspective on paleoproductivity variations in two Late Quaternary sediment sections from the Southeast Atlantic Ocean. Org. Geochem. 30, 341–366.
Hurrell, J.W., Kushnir, Y., Ottersen, G., Visbeck, M., 2003. An overview of the North Atlantic oscillation. In: Hurrell, J.W., Kushnir, Y., Ottersen, G., Visbeck, M. (Eds.), The North Atlantic Oscillation. American Geophysical Union, Washington, DC, pp. 1–35.
Incarbona, A., Bonomo, S., Di Stefano, E., Zgozi, S., Essarbout, N., Talha, M., Tranchida, G., Bonanno, A., Patti, B., Placenti, F., Buscaino, G., Cuttitta, A., Basilone, G., Bahri, T., Massa, F., Censi, P., Mazzola, S., 2008. Calcareous nannofossil surface sediment assemblages from the Sicily Channel (central Mediterranean Sea): palaeoceanographic implications. Mar. Micropaleontol. 67,

297–309.
Incarbona, A., Di Stefano, E., Sprovieri, R., Bonomo, S., Pelosi, N., Sprovieri, M., 2010. Millennial-scale paleoenvironmental changes in the central Mediterranean during the last interglacial: comparison with European and North Atlantic records. Geobios 43, 111–122.
Izdebski, A., 2016. In: Decker, M. (Ed.), Cambridge Companion to Byzantine Archaeology. Cambridge University Press, Cambridge (in press).
Izdebski, A., Koloch, G., Słoczyński, T., 2015. Exploring Byzantine and Ottoman economic history with the use of palynological data: a quantitative approach. Jahrb. Österreichischen Byz. 67–110.
Izdebski, A., Koloch, G., Słoczyński, T., Tycner-Wolicka, M., 2016. On the Use of palynological data in economic history: new methods and an Application to agricultural output in Central Europe, 0–2000 AD. Explor. Econ. Hist. 59, 17–39. http://dx.doi.org/10.1016/j.eeh.2015.10.003.
Josey, S.A., Somot, S., Tsimplis, M., 2011. Impacts of atmospheric modes of variability on Mediterranean Sea surface heat exchange. J. Geophys. Res. C Oceans 116.
Kaplan, A., Cane, M.A., Kushnir, Y., Clement, A.C., Blumenthal, M.B., Rajagopalan, B., 1998. Analyses of global sea surface temperature 1856–1991. J. Geophys. Res. C Oceans 103, 18,567–518,589.
Kaplan, M., 1992. Les hommes et la terre à Byzance du VIe au XIe siècle: propriété et exploitation du sol. Publications de la Sorbonne, Paris.
Katsouras, G., Gogou, A., Bouloubassi, I., Emeis, K.C., Triantaphyllou, M., Roussakis, G., Lykousis, V., 2010. Organic carbon distribution and isotopic composition in three records from the eastern Mediterranean Sea during the Holocene. Org. Geochem. 41, 935–939.
Kokoszko, M., Jagusiak, K., Rzeźnicka, Z., 2014. Cereals of Antiquity and Early Byzantine Times Wheat and Barley in Medical Sources (Second to Seventh Centuries AD), Byzantina Lodziensia. Łódź University Press, Łódź.
Kołaczek, P., Kupryjanowicz, M., Karpińska-Kołaczek, M., Szal, M., Winter, H., Danel, W., Pochocka-Szwarc, K., Stachowicz-Rybka, R., 2013. The Late Glacial and Holocene development of vegetation in the area of a fossil lake in the Skaliska Basin (north-eastern Poland) inferred from pollen analysis and radiocarbon dating. Acta Palaeobot. 23–52.
Kontoyiannis, H., Papadopoulos, V., Kazmin, A., Zatsepin, A., Georgopoulos, D., 2012. Climatic variability of the sub-surface sea temperatures in the Aegean-Black Sea system and relation to meteorological forcing. Clim. Dyn. 39, 1507–1525.
Kotthoff, U., Pross, J., Müller, U.C., Peyron, O., Schmiedl, G., Schulz, H., Bordon, A., 2008. Climate dynamics in the borderlands of the Aegean Sea during formation of sapropel S1 deduced from a marine pollen record. Quat. Sci. Rev. 27, 832–845.
Kouli, K., 2012. Vegetation development and human activities in Attiki (SE Greece) during the last 5,000 years. Veg. Hist. Archaeobot 21, 267–278.
Kouli, K., Gogou, A., Bouloubassi, I., Triantaphyllou, M.V., Ioakim, C., Katsouras, G., Roussakis, G., Lykousis, V., 2012. Late postglacial paleoenvironmental change in the northeastern Mediterranean region: combined palynological and molecular biomarker evidence. Quat. Int. 261, 118–127.
Kutiel, H., Maheras, P., Türkeş, M., Paz, S., 2002. North Sea – Caspian pattern (NCP) – an upper level atmospheric teleconnection affecting the eastern Mediterranean – implications on the regional climate. Theor. Appl. Climatol. 72, 173–192.
Laiou, A.E., 1977. Peasant Society in the Late Byzantine Empire. A Social and Demographical Study. Princeton University Press, Princeton, N.J.
Lascaratos, A., Roether, W., Nittis, K., Klein, B., 1999. Recent changes in deep water formation and spreading in the Eastern Mediterranean Sea: a review. Prog. Oceanogr. 44, 5–36.
Lefort, J., 1991a. L'organisation de l'espace rural: Macédoine et Italie du sud (Xe-XIIIe siècle). In: Hommes et Richesses Dans l'Empire Byzantin. Publications de la Sorbonne, Paris, pp. 11–26.
Lefort, J., 1991b. Population et peuplement en Macedoine orientale, IXe–XVe siecle. In: Hommes et Richesses Dans l'Empire Byzantin. Publications de la Sorbonne, Paris, pp. 69–71.
Lefort, J. (Ed.), 1986. Paysages de Macédoine: leurs caractères, leur évolution à travers les documents et les récits des voyageurs. De Boccard, Paris.
Lelieveld, J., Hadjinicolaou, P., Kostopoulou, E., Chenoweth, J., El Maayar, M., Giannakopoulos, C., Hannides, C., Lange, M.A., Tanarhte, M., Tyrlis, E., Xoplaki, E., 2012. Climate change and impacts in the Eastern Mediterranean and the Middle East. Clim. Change 114, 667–687.
Lemerle, P., 1979. Les plus anciens recueils des miracles de Saint Démétrius et la pénétration des Slaves dans les Balkans. Éditions du CNRS, Paris.
Lespez, L., 2003. Geomorphic responses to long-term land use changes in Eastern Macedonia (Greece). Catena 51, 181–208.
Lionello, P., Malanotte-Rizzoli, P., Boscolo, R., Alpert, P., Artale, V., Li, L., Luterbacher, J., May, W., Trigo, R., Tsimplis, M., Ulbrich, U., Xoplaki, E., 2006. The Mediterranean climate: an overview of the main characteristics and issues. Dev. Earth Environ. Sci. 1–26.
López-Parages, J., Rodríguez-Fonseca, B., 2012. Multidecadal modulation of El Niño influence on the Euro-Mediterranean rainfall. Geophys. Res. Lett. 39.
Luterbacher, J., Dietrich, D., Xoplaki, E., Grosjean, M., Wanner, H., 2004. European seasonal and annual temperature variability, trends, and extremes since 1500. Science 303, 1499–1503.
Luterbacher, J., García-Herrera, R., Akcer-On, S., Allan, R., Alvarez-Castro, M.C., Benito, G., Booth, J., Büntgen, U., Cagatay, N., Colombaroli, D., Davis, B., Esper, J., Felis, T., Fleitmann, D., Frank, D., Gallego, D., Garcia-Bustamante, E., Glaser, R., Gonzalez-Rouco, F.J., Goosse, H., Kiefer, T., Macklin, M.G., Manning, S.W., Montagna, P., Newman, L., Power, M.J., Rath, V., Ribera, P., Riemann, D., Roberts, N., Sicre, M.A., Silenzi, S., Tinner, W., Tzedakis, P., Valero-Garcés, B., van der Schrier, G., Vannière, B., Vogt, S., Wanner, H., Werner, J.P., Willett, G., Williams, M.H., Xoplaki, E., Zerefos, C.S., Zorita, E., 2012. A Review of 2000 Years of Paleoclimatic Evidence in the Mediterranean, the Climate of the Mediterranean Region. Elsevier Inc., pp. 87–185
Luterbacher, J., Xoplaki, E., 2003. 500-Year Winter temperature and precipitation variability over the mediterranean area and its connection to the large-scale atmospheric circulation. In: Bolle, H.-J. (Ed.), Mediterranean Climate. Variability and Trends. Springer Verlag, Berlin, Heidelberg, pp. 133–153.
Luterbacher, et al., 2016. European summer temperatures since Roman times. Environ. Res. Lett. 11, 024001. http://dx.doi.org/10.1088/1748-9326/11/1/024001.
Lykousis, V., Chronis, G., Tselepides, A., Price, N.B., Theocharis, A., Siokou-Frangou, I., Van Wambeke, F., Danovaro, R., Stavrakakis, S., Duineveld, G., Georgopoulos, D., Ignatiades, L., Souvermezoglou, A., Voutsinou-Taliadouri, F., 2002. Major outputs of the recent multidisciplinary biogeochemical researches undertaken in the Aegean Sea. J. Mar. Syst. 33–34, 313–334.
Malanotte-Rizzoli, P., Artale, V., Borzelli-Eusebi, G.L., Brenner, S., Crise, A., Gacic, M., Kress, N., Marullo, S., Ribera D'Alcalà, M., Sofianos, S., Tanhua, T., Theocharis, A., Alvarez, M., Ashkenazy, Y., Bergamasco, A., Cardin, V., Carniel, S., Civitarese, G., D'Ortenzio, F., Font, J., Garcia-Ladona, E., Garcia-Lafuente, J.M., Gogou, A., Gregoire, M., Hainbucher, D., Kontoyannis, H., Kovacevic, V., Kraskapoulou, E., Kroskos, G., Incarbona, A., Mazzocchi, M.G., Orlic, M., Ozsoy, E., Pascual, A., Poulain, P.M., Roether, W., Rubino, A., Schroeder, K., Siokou-Frangou, J., Souvermezoglou, E., Sprovieri, M., Tintoré, J., Triantafyllou, G., 2014. Physical forcing and physical/biochemical variability of the Mediterranean Sea: a review of unresolved issues and directions for future research. Ocean Sci. 10, 281–322.
Malinverno, E., Triantaphyllou, M.V., Stavrakakis, S., Ziveri, P., Lykousis, V., 2009. Seasonal and spatial variability of coccolithophore export production at the South-Western margin of Crete (Eastern Mediterranean). Mar. Micropaleontol. 71, 131–147.
Mann, M.E., Zhang, Z., Rutherford, S., Bradley, R.S., Hughes, M.K., Shindell, D., Ammann, C., Faluvegi, G., Ni, F., 2009. Global signatures and dynamical origins of the little ice age and medieval climate anomaly. Science 326, 1256–1260.
Marinova, E., Tonkov, S., Bozilova, E., Vajsov, I., 2012. Holocene anthropogenic landscapes in the Balkans: the palaeobotanical evidence from southwestern Bulgaria. Veg. Hist. Archaeobot. 21, 413–427.
Mariotti, A., Dell'Aquila, A., 2012. Decadal climate variability in the Mediterranean region: Roles of large-scale forcings and regional processes. Clim. Dyn. 38, 1129–1145.
Marlowe, I.T., Green, J.C., Neal, A.C., Brassell, S.C., Eglinton, G., Course, P.A., 1984. Long chain (n-C37-C39) alkenones in the Prymnesiophyceae. Distribution of alkenones and other lipids and their taxonomic significance. Br. Phycol. J. 19, 203–216.
Marullo, S., Artale, V., Santoleri, R., 2011. The SST multidecadal variability in the Atlantic-Mediterranean region and its relation to AMO. J. Clim. 24, 4385–4401.
McGowan, B., 1981. Economic Life in Ottoman Europe: Taxation, Trade, and the Struggle for Land, 1600–1800. Cambridge University Press, Cambridge.
Medina-Elizalde, M., Rohling, E., 2012. Collapse of classic maya civilization related to modest reduction in precipitation. Science 335 (6071), 956–959. http://dx.doi.org/10.1126/science.1216629.
Menzel, D., Van Bergen, P.F., Schouten, S., Sinninghe Damsté, J.S., 2003. Reconstruction of changes in export productivity during pliocene sapropel deposition: a biomarker approach. Palaeogeogr. Palaeoclimatol. Palaeoecol. 190, 273–287.
Mercuri, A.M., Bandini Mazzanti, M., Florenzano, A., Montecchi, M.C., Rattighieri, E., 2013a. Olea, Juglans and Castanea: the OJC group as pollen evidence of the development of human-induced environments in the Italian peninsula. Quat. Int. 303, 24–42.
Mercuri, A.M., Bandini Mazzanti, M., Florenzano, A., Montecchi, M.C., Rattighieri, E., Torri, P., 2013b. Anthropogenic pollen indicators (API) from archaeological sites as local evidence of human-induced environments in the Italian Peninsula. Ann. Di Bot. 3, 143–153.
Mercuri, A.M., Sadori, L., 2014. Mediterranean culture and climatic change: past patterns and future trends. In: Goffredo, S., Dubinsky, Z. (Eds.), The Mediterranean Sea: its History and Present Challenges. Springer, Dordrecht, pp. 507–527.
Molfino, B., McIntyre, A., 1990. Precessional forcing of nutricline dynamics in the equatorial Atlantic. Science 249, 766–769.
Moore, G.W.K., Pickart, R.S., Renfrew, I.A., 2011. Complexities in the climate of the subpolar North Atlantic: a case study from the winter of 2007. Q. J. R. Meteorological Soc. 137, 757–767.
Moreno, A., Pérez, A., Frigola, J., Nieto-Moreno, V., Rodrigo-Gámiz, M., Martrat, B., González-Sampériz, P., Morellón, M., Martín-Puertas, C., Corella, J.P., Belmonte, Á., Sancho, C., Cacho, I., Herrera, G., Canals, M., Grimalt, J.O., Jiménez-Espejo, F., Martínez-Ruiz, F., Vegas-Vilarrúbia, T., Valero-Garcés, B.L., 2012. The Medieval Climate Anomaly in the Iberian Peninsula reconstructed from marine and lake records. Quat. Sci. Rev. 43, 16–32.
Negri, A., Giunta, S., 2001. Calcareous nannofossil paleoecology in the sapropel S1 of the Eastern Ionian sea: paleoceanographic implications. Palaeogeogr. Palaeoclimatol. Palaeoecology 169, 101–112.
Nieto-Moreno, V., Martínez-Ruiz, F., Willmott, V., García-Orellana, J., Masqué, P., Sinninghe Damsté, J.S., 2013. Climate conditions in the westernmost Mediterranean over the last two millennia: an integrated biomarker approach. Org. Geochem. 55, 1–10.
Odorico, P., 2005. Thessalonique: Chroniques D'une Ville Prise. Anacharsis, Toulouse.

Ohkouchi, N., Kawamura, K., Kawahata, H., Taira, A., 1997. Latitudinal distributions of terrestrial biomarkers in the sediments from the Central Pacific. Geochimica Cosmochimica Acta 61, 1911–1918.
Okada, H., Honjo, S., 1973. Distribution of oceanic coccolithophorids in the Pacific. Deep Sea Res. 20, 355–374.
Oppenheimer, C., 2003. Climatic, environmental and human con sequences of the largest known historic eruption: Tambora volcano (Indonesia) 1815. Prog. Phys. Geogr. 27, 230–259.
Ortega, P., Lehner, F., Swingedouw, D., Masson-Delmotte, D., Raible, C.C., Casado, M., Yiou, P., 2015. A model-tested North Atlantic Oscillation reconstruction for the past millennium. Nature 523, 71–74.
Ouyang, X., Guo, F., Bu, H., 2015. Lipid biomarkers and pertinent indices from aquatic environment record paleoclimate and paleoenvironment changes. Quat. Sci. Rev. 123, 180–192.
Palumbo, E., Flores, J.A., Perugia, C., Petrillo, Z., Voelker, A.H.L., Amore, F.O., 2013. Millennial scale coccolithophore paleoproductivity and surface water changes between 445 and 360 ka (Marine Isotope Stages 12/11) in the Northeast Atlantic. Palaeogeogr. Palaeoclimatol. Palaeoecol. 383–384, 27–41.
Papadopoulos, V.P., Kontoyiannis, H., Ruiz, S., Zarokanellos, N., 2012. Influence of atmospheric circulation on turbulent air-sea heat fluxes over the Mediterranean Sea during winter. J. Geophys. Res. C Oceans 117.
Parinos, C., Gogou, A., Bouloubassi, I., Pedrosa-Pàmies, R., Hatzianestis, I., Sanchez-Vidal, A., Rousakis, G., Velaoras, D., Krokos, G., Lykousis, V., 2013. Occurrence, sources and transport pathways of natural and anthropogenic hydrocarbons in deep-sea sediments of the eastern Mediterranean Sea. Biogeosciences 10, 6069–6089.
Parker, D.E., Folland, C.K., Jackson, M., 1995. Marine surface temperature: observed variations and data requirements. Clim. Change 31, 559–600.
Pauling, A., Luterbacher, J., Casty, C., Wanner, H., 2006. Five hundred years of gridded high-resolution precipitation reconstructions over Europe and the connection to large-scale circulation. Clim. Dyn. 26, 387–405.
Peyron, O., Goring, S., Dormoy, I., Kotthoff, U., Pross, J., de Beaulieu, J.L., Drescher-Schneider, R., Vanniére, B., Magny, M., 2011. Holocene seasonality changes in the central mediterranean region reconstructed from the pollen sequences of Lake Accesa (Italy) and Tenaghi philippon (Greece). Holocene 21, 131–146.
Peyron, O., Magny, M., Goring, S., Joannin, S., De Beaulieu, J.L., Brugiapaglia, E., Sadori, L., Garfi, G., Kouli, K., Ioakim, C., Combourieu-Nebout, N., 2013. Contrasting patterns of climatic changes during the Holocene across the Italian Peninsula reconstructed from pollen data. Clim. Past. 9, 1233–1252.
Pinardi, N., Zavatarelli, M., Adani, M., Coppini, G., Fratianni, C., Oddo, P., Simoncelli, S., Tonani, M., Lyubartsev, V., Dobricic, S., Bonaduce, A., 2015. Mediterranean Sea large-scale low-frequency ocean variability and water mass formation rates from 1987 to 2007: a retrospective analysis. Prog. Oceanogr. 132, 318–332. http://dx.doi.org/10.1016/j.pocean.2013.11.003.
Popović, M., 2012. Spätbyzantinische Siedlungen und wlachische Transhumanz in den Flusstälern der Strumica und Kriva Lakavica. In: Dahmen, W. (Ed.), Südosteuropäische Romania: Siedlungs-/Migrationsgeschichte Und Sprachtypologie. Romanistisches Kolloquium XXV, Tübinger Beiträge Zur Linguistik. Narr, Tübingen, pp. 227–240.
Poulos, S.E., Drakopoulos, P.G., Collins, M.B., 1997. Seasonal variability in sea surface oceanographic conditions in the Aegean Sea (Eastern Mediterranean): an overview. J. Mar. Syst. 13, 225–244.
Poynter, J., Eglinton, G., 1990. Molecular composition of three sediments from hole 717C: the Bengal Fan. In: Proc., scientific results, ODP, Leg. 116, distal Bengal Fan, pp. 155–161.
Radakovitch, O., 1995. Etude du transfert et du depot du materiel particulaire par le 210Po et le 210Pb. Application aux marges continentales du Golfe de Gascogne (NE Atlantique) et du Golfe du Lion (NW Mediterranee). Ph.D. Thesis. University of Perpignan.
Raduschev, E., 2005. The “besieged” mountains. Bulg. Hist. Rev. 33, 17–58.
Raible, C.C., Brönnimann, S., Auchmann, R., Brohan, P., Frölicher, T., Graf, H.F., Jones, P.D., Luterbacher, J., Muthers, S., Robock, A., Self, S., Sudrajat, A., Timmreck, C., Wegmann, M., 2016. Tambora 1815 as a test case for high impact volcanic eruptions: earth system effects. Wires Clim. Change in press.
Rampen, S.W., Schouten, S., Koning, E., Brummer, G.J.A., Sinninghe Damsté, J.S., 2008. A 90 kyr upwelling record from the northwestern Indian Ocean using a novel long-chain diol index. Earth Planet. Sci. Lett. 276, 207–213.
Reimer, P.J., Bard, E., Bayliss, A., Beck, J.W., Blackwell, P.G., Bronk Ramsey, C., Buck, C.E., Cheng, H., Edwards, R.L., Friedrich, M., Grootes, P.M., Guilderson, T.P., Haflidason, H., Hajdas, I., Hatté, C., Heaton, T.J., Hoffmann, D.L., Hogg, A.G., Hughen, K.A., Kaiser, K.F., Kromer, B., Manning, S.W., Niu, M., Reimer, R.W., Richards, D.A., Scott, E.M., Southon, J.R., Staff, R.A., Turney, C.S.M., van der Plicht, J., 2013. IntCal13 and Marine13 radiocarbon age calibration curves 0-50,000 years cal BP. Radiocarbon 55, 1869–1887.
Reimer, P.J., McCormac, F.G., 2002. Marine radiocarbon reservoir corrections for the Mediterranean and Aegean Seas. Radiocarbon 44, 159–166.
Repeta, D.J., 1989. Carotenoid diagenesis in recent marine sediments: II. Degradation of fucoxanthin to loliolide. Geochimica Cosmochimica Acta 53, 699–707.
Reynolds, R.W., Smith, T.M., 1994. Improved global sea surface temperature analyses using optimum interpolation. J. Clim. 7, 929–948.
Ribera, P., Garcia, R., Diaz, H.F., Gimeno, L., Hernandez, E., 2000. Trends and interannual oscillations in the main sea-level surface pressure patterns over the Mediterranean, 1955–1990. Geophys. Res. Lett. 27, 1143–1146.
Ritter, M., 2013. Die vlacho-bulgarische Rebellion und die Versuche ihrer Niederschlagung durch Kaiser Isaakios II. (1185–1195). Byzantinoslavica 71, 162–210.
Roberts, N., Brayshaw, D., Kuzucuoğlu, C., Perez, R., Sadori, L., 2011. The mid-Holocene climatic transition in the Mediterranean: causes and consequences. Holocene 21, 3–13.
Roberts, N., Moreno, A., Valero-Garcés, B.L., Corella, J.P., Jones, M., Allcock, S., Woodbridge, J., Morellón, M., Luterbacher, J., Xoplaki, E., Türkeş, M., 2012. Palaeolimnological evidence for an east-west climate see-saw in the Mediterranean since AD 900. Glob. Planet. Change 84–85, 23–34.
Robinson, S.A., Black, S., Sellwood, B.W., Valdes, P.J., 2006. A review of palaeoclimates and palaeoenvironments in the Levant and Eastern Mediterranean from 25,000 to 5000 years BP: setting the environmental background for the evolution of human civilization. Quat. Sci. Rev. 25, 1517–1541. http://dx.doi.org/10.1016/j.quascirev.2006.02.006.
Robock, A., Jianping, M., 1995. The volcanic signal in surface temperature observations. J. Clim. 8, 1086–1103.
Rodrigo-Gámiz, M., Martínez-Ruiz, F., Rampen, S.W., Schouten, S., Sinninghe Damsté, J.S., 2014. Sea surface temperature variations in the western Mediterranean Sea over the last 20 kyr: A dual-organic proxy (UK' 37 and LDI) approach. Paleoceanography 29, 87–98.
Roether, W., Manca, B.B., Klein, B., Bregant, D., Georgopoulos, D., Beitzel, V., Kovačević, V., Luchetta, A., 1996. Recent changes in eastern Mediterranean deep waters. Science 271, 333–335.
Rohling, E.J., Marino, G., Grant, K.M., 2015. Mediterranean climate and oceanography, and the periodic development of anoxic events (sapropels). Earth Sci. Rev. 143, 62–97.
Romanski, J., Romanou, A., Bauer, M., Tselioudis, G., 2012. Atmospheric forcing of the eastern mediterranean transient by midlatitude cyclones. Geophys. Res. Lett. 39, L03703.
Roussakis, G., Karageorgis, A.P., Conispoliatis, N., Lykousis, V., 2004. Last glacial-Holocene sediment sequences in N. Aegean basins: structure, accumulation rates and clay mineral distribution. Geo-Mar. Lett. 24, 97–111.
Sadori, L., Giraudi, C., Masi, A., Magny, M., Ortu, E., Zanchetta, G., Izdebski, A., Climate, environment and society in Southern Italy during the last 2000 years, 2015. A review of the environmental, historical and archaeological evidence. Quat. Sci. Rev. http://dx.doi.org/10.1016/j.quascirev.2015.09.020.
Sanchez-Cabeza, J.A., Masque, P., Ani-Ragolta, I., 1998. 210Pb and 210Po analysis in sediments and soils by microwave acid digestion. J. Radioanalytical Nucl. Chem. 227, 19–22.
Schlesinger, R.E., 1994. Heat, moisture, and momentum budgets of isolated deep midlatitude and tropical convective clouds as diagnosed from three-dimensional model output. Part I: control experiments. J. Atmos. Sci. 51, 3649–3673.
Schmid, B.V., Büntgen, U., Easterday, W.R., Ginzler, C., Walløe, L., Bramanti, B., Stenseth, N.C., 2015. Climate-driven introduction of the Black Death and successive plague reintroductions into Europe. Proc. Natl. Acad. Sci. U. S. A. http://dx.doi.org/10.1073/pnas.1412887112.
Skliris, N., Sofianos, S., Gkanasos, A., Mantziafou, A., Vervatis, V., Axaopoulos, P., Lascaratos, A., 2012. Decadal scale variability of sea surface temperature in the Mediterranean Sea in relation to atmospheric variability. Ocean. Dyn. 62, 13–30.
Stothers, R.B., 1984. The Great Tambora eruption in 1815 and its aftermath. Science 224, 1191–1198.
Strong, D., Flecker, R., Valdes, P.J., Wilkinson, I.P., Rees, J.G., Michaelides, K., Zong, Y.Q., Lloyd, J.M., Yu, F.L., Pancost, R.D., 2013. A new regional, mid-Holocene palaeoprecipitation signal of the Asian Summer Monsoon. Quat. Sci. Rev. 78, 65–76.
Theocharis, A., Georgopoulos, D., 1993. Dense water formation over the Samothraki and Limnos plateaux in the north aegean sea (Eastern mediterranean sea). Cont. Shelf Res. 13, 919–939.
Theocharis, A., Krokos, G., Velaoras, D., Korres, G., 2014. An Intern. Mech. Driv. Altern. East. Mediterr. dense/deep water sources. In: Borzelli, G.L.E., Gačić, M., Lionello, P., Malanotte-Rizzoli, P. (Eds.), The Mediterranean Sea: Temporal Variability and Spatial Patterns, AGU Geophysical Monograph Series, 202. John Wiley & Sons., Inc., Oxford, U.K, pp. 113–137.
Theocharis, A., Nittis, K., Kontoyiannis, H., Papageorgiou, E., Balopoulos, E., 1999. Climatic changes in the Aegean Sea influence the Eastern Mediterranean thermohaline circulation (1986–1997). Geophys. Res. Lett. 26, 1617–1620.
Triantaphyllou, M.V., 2014. Coccolithophore assemblages during the Holocene Climatic Optimum in the NE Mediterranean (Aegean and northern Levantine Seas, Greece): paleoceanographic and paleoclimatic implications. Quat. Int. 345, 56–67.
Triantaphyllou, M.V., Ziveri, P., Tselepides, A., 2004. Coccolithophore export production and response to seasonal surface water variability in the oligotrophic Cretan Sea (NE Mediterranean). Micropaleontology 50, 127–144.
Triantaphyllou, M.V., Antonarakou, A., Kouli, K., Dimiza, M., Kontakiotis, G., Papanikolaou, M.D., Ziveri, P., Mortyn, P.G., Lianou, V., Lykousis, V., Dermitzakis, M.D., 2009a. Late Glacial-Holocene ecostratigraphy of the south-eastern Aegean Sea, based on plankton and pollen assemblages. Geo-Mar. Lett. 29, 249–267.
Triantaphyllou, M.V., Ziveri, P., Gogou, A., Marino, G., Lykousis, V., Bouloubassi, I., Emeis, K.C., Kouli, K., Dimiza, M., Rosell-Melé, A., Papanikolaou, M., Katsouras, G., Nunez, N., 2009b. Late Glacial-Holocene climate variability at the south-eastern margin of the Aegean Sea. Mar. Geol. 266, 182–197.
Triantaphyllou, M.V., Kouli, K., Tsourou, T., Koukousioura, O., Pavlopoulos, K., Dermitzakis, M.D., 2010. Paleoenvironmental changes since 3000 BC in the coastal marsh of Vravron (Attica, SE Greece). Quat. Int. 216, 14–22.

Triantaphyllou, M.V., Gogou, A., Bouloubassi, I., Dimiza, M., Kouli, K., Rousakis, G., Kotthoff, U., Emeis, K.C., Papanikolaou, M., Athanasiou, M., Parinos, C., Ioakim, C., Lykousis, V., 2014. Evidence for a warm and humid Mid-Holocene episode in the Aegean and northern Levantine Seas (Greece, NE Mediterranean). Reg. Environ. Change 14, 1697–1712.

Triantaphyllou, M.V., Gogou, A., Dimiza, M.D., Kostopoulou, S., Parinos, C., Roussakis, G., Geraga, M., Bouloubassi, I., Fleitmann, D., Zervakis, V., Velaoras, D., Diamantopoulou, A., Sampatakaki, A., Lykousis, V., 2016. Holocene climatic optimum centennial-scale paleoceanography in the NE Aegean (Mediterranean Sea). Geo-Mar. Lett. 36, 51–66.

Turner, S., 2004. Vitis pollen dispersal in and from organic vineyards I. Pollen trap and soil pollen data. Rev. Palaeobot. Palynology 129, 117–132.

Ulbrich, U., Xoplaki, E., Dobricic, S., García-Herrera, R., Lionello, P., et al., 2013. Past and current climate changes in the Mediterranean Region. In: Navarra, A., Tubiana, L. (Eds.), Regional Assessment of Climate Change in the Mediterranean, Advances in Global Change Research, vol. 50. Springer, Netherlands, pp. 9–50. ISBN: 978-94-007-5780-6 (Print) 978-94-007-5781-3 (Online).

Van Geel, B., Coope, G.R., Van Der Hammen, T., 1989. Palaeoecology and stratigraphy of the lateglacial type section at Usselo (the Netherlands). Rev. Palaeobot. Palynology 60, 25-38,41-42,45-46,48-49,51-60,63-64,67-68,75–129.

Velaoras, D., Kassis, D., Perivoliotis, L., Pagonis, P., Hondronasios, A., Nittis, K., 2013. Temperature and salinity variability in the greek seas based on POSEIDON stations time series: preliminary results. Mediterr. Mar. Sci. 14, 5–18.

Velaoras, D., Krokos, G., Nittis, K., Theocharis, A., 2014. Dense intermediate water outflow from the Cretan Sea: a salinity driven, recurrent phenomenon, connected to thermohaline circulation changes. J. Geophys. Res. Oceans 119, 4797–4820.

Velaoras, D., Lascaratos, A., 2005. Deep water mass characteristics and interannual variability in the North and Central Aegean Sea. J. Mar. Syst. 53, 59–85.

Velaoras, D., Lascaratos, A., 2010. North-Central Aegean Sea surface and intermediate water masses and their role in triggering the Eastern Mediterranean Transient. J. Mar. Syst. 83, 58–66.

Versteegh, G.J.M., De Leeuw, J.W., Taricco, C., Romero, A., 2007. Temperature and productivity influences on U37 K′ and their possible relation to solar forcing of the Mediterranean winter. Geochem. Geophys. Geosystems 8.

Volkman, J.K., 1986. A review of sterol markers for marine and terrigenous organic matter. Org. Geochem. 9, 83–99.

Volkman, J.K., Barrett, S.M., Blackburn, S.I., 1999. Eustigmatophyte microalgae are potential sources of C 29 sterols, C 22-C 28 n-alcohols and C 28-C 32 n-alkyl diols in freshwater environments. Org. Geochem. 30, 307–318.

Wagner, S., Zorita, E., 2005. The influence of volcanic, solar and CO_2 forcing on the temperatures in the Dalton Minimum (1790–1830): a model study. Clim. Dyn. 25, 205–218.

Wand, M.P., Jones, M.C., 1995. Kernel Smoothing. CRC Press, USA.

Wang, Z., Fingas, M., Page, D.S., 1999. Oil spill identification. J. Chromatogr. A 843, 369–411.

Weiberg, E., Kouli, K., Unkel, I., Holmgren, K., et al., 2016. The socio-environmental history of the Peloponnese during the Holocene: towards an integrated understanding of the past. Quat. Sci. Rev. this issue.

Wegmann, M., Brönnimann, S., Bhend, J., Franke, J., Folini, D., Wild, M., Luterbacher, J., 2014. Influence of tropical volcanic eruptions on regional precipitation. J. Clim. 27, 3683–3691.

White, S., 2011. The Climate of Rebellion in the Early Modern Ottoman Empire, Studies in Environment and History. Cambridge University Press, Cambridge.

Winter, A., Jordan, R.W., Roth, P.H., 1994. Biogeography of living coccolithophores in ocean waters. In: Winter, A., Siesser, W.G. (Eds.), Coccolithophores. Cambridge University Press, New York, pp. 161–178.

Xoplaki, E., Fleitmann, D., Izdebski, A., Luterbacher, J., Wagner, S., Zorita, E., Telelis, I., Toreti, A., 2016. The Medieval Climate Anomaly and Byzantium; a review of evidence on climatic fluctuations, economic performance and societal change. Quat. Sci. Rev. http://dx.doi.org/10.1016/j.quascirev.2015.10.004 this issue.

Xoplaki, E., González-Rouco, J.F., Gyalistras, D., Luterbacher, J., Rickli, R., Wanner, H., 2003a. Interannual summer air temperature variability over Greece and its connection to the large-scale atmospheric circulation and Mediterranean SSTs 1950–1999. Clim. Dyn. 20, 537–554.

Xoplaki, E., González-Rouco, J.F., Luterbacher, J., Wanner, H., 2003b. Mediterranean summer air temperature variability and its connection to the large-scale atmospheric circulation and SSTs. Clim. Dyn. 20, 723–739.

Xoplaki, E., González-Rouco, J.F., Luterbacher, J., Wanner, H., 2004. Wet season Mediterranean precipitation variability: Influence of large-scale dynamics and trends. Clim. Dyn. 23, 63–78.

Xoplaki, E., Luterbacher, J., Paeth, H., Dietrich, D., Steiner, N., Grosjean, M., Wanner, H., 2005. European spring and autumn temperature variability and change of extremes over the last half millennium. Geophys. Res. Lett. 32, L15713.

Young, J.R., 1994. Functions of coccoliths. Coccolithophores 63–82.

Zervakis, V., Georgopoulos, D., Drakopoulos, P.G., 2000. The role of the North Aegean in triggering the recent Eastern Mediterranean climatic changes. J. Geophys. Res. C Oceans 105, 26103–26116.

Zervakis, V., Georgopoulos, D., Karageorgis, A.P., Theocharis, A., 2004. On the response of the Aegean Sea to climatic variability: a review. Int. J. Climatol. 24, 1845–1858.

Zervakis, V., Krasakopoulou, E., Georgopoulos, D., Souvermezoglou, E., 2003. Vertical diffusion and oxygen consumption during stagnation periods in the deep North Aegean. Deep-Sea Res. Part I Oceanogr. Res. Pap. 50, 53–71.